Spring 2011

Shape reconstruction and classification using the response matrix

Wei Wang

SHAPE RECONSTRUCTION AND CLASSIFICATION USING THE RESPONSE MATRIX

by

Wei Wang, B S , M S

A Dissertation Presented in Partial Fulfillment
of the Requirements for the Degree
Doctor of Philosophy

COLLEGE OF ENGINEERING AND SCIENCE
LOUISIANA TECH UNIVERSITY

May 2011

LOUISIANA TECH UNIVERSITY

THE GRADUATE SCHOOL

04/07/2011

Date

We hereby recommend that the dissertation prepared under our supervision by Wei Wang

entitled Shape Reconstruction and Classification using the Response Matrix

be accepted in partial fulfillment of the requirements for the Degree of Ph D in Computational Analysis and Modeling

Supervisor of Dissertation Research

Head of Department

Computational Analysis and Modeling

Department

Recommendation concurred in

Advisory Committee

Approved

Director of Graduate Studies

Dean of the College

Approved

Dean of the Graduate School

GS Form 13a
(6/07)

ABSTRACT

This dissertation presents a novel method for the inverse scattering problem for extended target The acoustic or electromagnetic wave is scattered by the target and received by all the transducers around the target The scattered field on all the transducers forms the response matrix which contains the information of the geometry of the target The objective of the inverse scattering problem is to reconstruct the shape of the scatter using the Response Matrix

There are two types of numerical methods for solving the inverse problem the direct imaging method and the iterative method Two direct imaging methods, MUSIC method and Multi-tone method, are introduced in this dissertation The direct imaging method generates the image, which contains the shape of the target, by defining the image function using the response matrix Numerical examples show that the two direct imaging methods are efficient and robust, and the Multi-tone method can be used in synthetic aperture

The iterative method described in this dissertation achieves better accuracy than the direct imaging method The result of the direct imaging method of the inverse problem is used as an initial estimation for this iterative method One forward problem and one adjoint problem is solved in each iteration step Numerical results show that the residual vanishes at a fixed wave number The final result after iterations is more accurate than the result from the direct imaging method

This dissertation also introduces the application of the inverse problem shape identification and classification The response matrix used in shape classification can be generated by the forward solver or Born approximation The distance function designed using a response matrix or its SVD information is effective and robust to noise The classification method using the response matrix is tested on a large data set and compared with other classification algorithms on the retrieval accuracy

APPROVAL FOR SCHOLARLY DISSEMINATION

The author grants to the Prescott Memorial Library of Louisiana Tech University the right to reproduce, by appropriate methods, upon request, any or all portions of this Dissertation It is understood that "proper request" consists of the agreement, on the part of the requesting party, that said reproduction is for his personal use and that subsequent reproduction will not occur without written approval of the author of this Dissertation Further, any portions of the Dissertation used in books, papers, and other works must be appropriately referenced to this Dissertation

Finally, the author of this Dissertation reserves the right to publish freely, in the literature, at any time, any or all portions of this Dissertation

Author Wang Wei

Date 05/03/2011

GS Form 14
(5/03)

DEDICATION

This dissertation is dedicated to my parents for their unconditional love and support all the way in my life

TABLE OF CONTENTS

LIST OF FIGURES

NOMENCLATURE

u	the total field
$u^{\imath}$	the incident field
u^{s}	the scattered field
P	the response matrix
k	the wave number
c	the speed of sound
r	the distance
D	the impenetrable obstacle
Ω	the medium region
$\mathbb{R}$	the real space
$\mathbb{C}$	the complex space
$\imath$	the imaginary unit
ν	the unit outward normal
v	the velocity field
ρ	the density
p	the pressure
ω	the wave frequency

Φ	the fundamental solution of Helmholtz equation
φ	the density function
ψ	the discrete density function
S	the single-layer operator
K	the double-layer operator
η	the coupling parameter
K', T	the normal derivative operator
L, M	the integral kernel
$n(\ )$	the index of refraction
$G(\ ,\ )$	the Green's function
$G_0(\ ,\ )$	the homogeneous Green's function
$G_D(\ ,\ )$	the inhomogeneous Green's function
$\vec{g}_0(\ )$	the homogeneous illumination vector
$\vec{g}_D(\ )$	the inhomogeneous illumination vector
V_S	the signal space
P_{V_S}	the projection operator
I	the identity operator
$I^M(\ )$	the imaging function
Γ_k	the scatter at wave number k
$\mathcal{M}$	the measurement operator

$\mathcal{F}$	the forward scattering operator
$\mathcal{R}$	the residual operator
a	the velocity vector
β	the positive relaxation parameter
$\delta(\,)$	the delta function
ϕ	the level set function
Δ	the Laplace operator
∇	the gradient operator
w	the solution of adjoint problem

ACKNOWLEDGEMENTS

I would like to thank my advisor, Dr Songming Hou, for his guidance and coordination during my Ph D program As a mentor and a friend, Dr Hou gave me generous help and precious advice in my life and research

I thank the professors of my academic committee, Dr Weizhong Dai, Dr Don Liu, Dr Andrei Paun, and Dr Mihaela Paun, for their valuable feedbacks about this dissertation

I am also grateful to the professors of Louisiana Tech, who gave me comprehensive knowledge during the past three academic years I have benefited so much from their courses and constant encouragement

Many thanks to my colleagues at Louisiana Tech Liqun Wang gave me a lot of help in my daily life and course work We cooperated on many projects and shared the happiness of research I also thank Lisa Kuhn for her help and encouragement Finally, my gratitude goes to all of my friends in Ruston for their constant support and concern

CHAPTER 1

INTRODUCTION

1 1 The Direct Scattering Problem

Scattering theory has played a central role in twentieth century mathematical physics The incoming acoustic or electromagnetic wave can be scattered by the target in the center of the domain and received by the transducers around the object Let u be the total field, u^i be the incident field coming from one position or one direction, and u^s be the scattered field The total field u can be viewed as the summation of u^i and u^s such that

$$u = u^i + u^s \tag{1 1}$$

The direct scattering problem is to determine u^s from a knowledge of u^i, the shape information of the target, and the differential equation governing the wave motion, see [5, 11, 20, 29, 30, 33, 34, 39, 44]

The two basic problems in classical scattering theory are the scattering of time-harmonic acoustic or electromagnetic waves by a penetrable inhomogeneous medium of compact support and by a bounded impenetrable obstacle

Considering the case of time-harmonic acoustic waves, assume the incident field is given by the time-harmonic acoustic plane wave

$$u^i(x,t) = e^{i(kx\ d-\omega t)}, \tag{1 2}$$

where $k = \omega/c_0$ is the wave number, ω the frequency, c_0 the speed of sound, and d the direction of propagation

Then the scattering problem for the case of an inhomogeneous medium is to find the total field u such that

$$\Delta u + k^2 n(x) u = 0 \qquad \text{in } \mathbb{R}^3, \tag{1 3}$$

$$u(x) = e^{ikx\, d} + u^s(x), \tag{1 4}$$

$$\lim_{r\to\infty} r\left(\frac{\partial u^s}{\partial r} - iku^s\right) = 0, \tag{1 5}$$

where $r = \|x\|$, $n = c_0^2/c^2$ is the refractive index given by the ratio of the square of the sound speed c, which satisfies that $c = c_0$ in the homogeneous host medium and $c = c(x)$ in the inhomogeneous medium It is assumed that $1 - n$ has compact support Equation (1 5) is called the **Sommerfeld Radiation Condition** which guarantees that the scattered wave is outgoing

For the case of scattering by an impenetrable obstacle D, the simplest scattering problem is to find the total field u such that

$$\Delta u + k^2 n(x) u = 0 \qquad \text{in } \mathbb{R}^3 \backslash \overline{D}, \tag{1 6}$$

$$u(x) = e^{ikx\, d} + u^s(x), \tag{1 7}$$

$$u = 0 \qquad \text{on } \partial D, \tag{1 8}$$

$$\lim_{r\to\infty} r\left(\frac{\partial u^s}{\partial r} - iku^s\right) = 0, \tag{1 9}$$

where the Equation (1 6) is the **Helmholtz equation** and the boundary condition, Equation (1 8), corresponds to a *sound-soft* obstacle The boundary condition can also be considered for the Neumann or *sound-hard* boundary condition

$$\frac{\partial u}{\partial \nu} = 0 \qquad \text{on } \partial D, \tag{1 10}$$

where ν is the unit outward normal to ∂D

Problems from Equation (1 3)-(1 5) and Equation (1 6)-(1 9) are the simplest examples of physically realistic problems in acoustic scattering theory More details about the scattering theory can be found in [12] This dissertation is primarily concerned with the inverse scattering problems associated with the direct scattering problems formulated above However, before the inverse problems can be considered, more about the direct problems must be studied Chapter 2 focuses on the details of direct scattering problems and introduces the numerical method for solving direct scattering problems in $\mathbb{R}^2$, which will be used in the iterative method of inverse problems

1 2 The Inverse Scattering Problem

For the inverse scattering problem, the refractive index $n(x)$ or the geometry of target D is unknown The information of incident waves is given and the scattered waves is recorded by the transducers The objective is to find the location and geometry of the targets, which is determined by $n(x)$ or D, using the the relation between incident waves and scattered outgoing waves

The inverse scattering problems is widely used in industry such as

1 underground mine detection

2 detection of defects in nondestructive testing,

3 target detection using radar or a sonar system,

4 ultrasound imaging in medical applications,

5 reflection seismology

The inverse problem is in general an ill-posed (non-linear) problem Recovering the $n(x)$ in the whole domain is a challenging work If the target medium is homogeneous the $n(x)$ is a constant inside the target, then the inverse problem can be turned into a geometric problem, which is to reconstruct the shape of the target D

There are essentially two types of numerical methods for the inverse problem the direct imaging method and the iterative method The direct method gives a characterization of the geometry of the target by designing an imaging function based on the response matrix that peaks near the target boundary Iterative methods update the boundary of the target to minimize the residual of the scattered field It is a nonlinear optimization process

Based on the relation between the resolution and the size of the target, there are two different cases point target and extended target The MUltiple SIgnal Classification (MUSIC) method in [13, 15, 22, 37, 40] can be used to locate small target (point target) The authors in [38, 36, 42, 43, 21] use iterated time reversal to recover small target The MUSIC algorithm is generalized to applied on extended targets for near field data in [18], and for far field data in [19]

The MUSIC method is efficient and robust It, however, cannot generate good result for limited or synthetic aperture since it uses single frequency to capture the shape and the projection process loses the phase information of the response matrix In [16], the author proposed a Multi-tone imaging algorithm that uses both phase and space information of the response matrix, and utilizes multiple frequency waves

The linear sampling method, [10], is another direct imaging algorithm for the inverse scattering problem The method is based on a characterization of the range of the scattering operator, which is presented in [24] Recent development of the linear sampling method is introduced in [4, 9] There are two main differences between the MUSIC method and the linear sampling method

1 The MUSIC method is based on a different factorization

2 The MUSIC method uses the resolution based thresholding for regularization

More details about the relation between the MUSIC method and the linear sampling method can be found in [7, 25]

The iterative method for the inverse problem is the main purpose of this dissertation The iterative method is a non-linear optimization approach It has the advantage of accuracy compared to the direct imaging method Moreover, the iterative method can easily utilize multi-frequency date to capture multi-level details of the object Using the forward solver, each iteration step contains a forward scattering problem and an adjoint problem The forward solver can be parallelized to increase the iteration speed In Chapter 4, the iterative method will be demonstrated starting from the initial data, which is obtained by the direct imaging method The shape of the object converges to the real shape after a series of iterations of solving adjoint forward problems and adjusting the boundary

Shape identification and classification using scattered field data is an application of the inverse problem Shape classification and similarity are important topics in computer vision In [45], the author presented a skeleton graph matching method based on critical points using path similarity This method uses information from critical points of the skeleton graph of shapes, then does merge and cut operations Good results are achieved on two shape data-sets Another method to generate the response matrix is using the Poisson Equation [14] The authors use the information from the silhouette for shape recognition and classification by computing properties of a silhouette such as the part structure, the rough skeleton and the local orientation In [1], the author provided a distance function by using the shortest paths or distances between the known shapes and their query, and ignoring less relevant shape differences between the known shapes and their query

The current method for shape classification uses the response matrix generated by the Nystrom method of forward solver or Born approximation Shape space is geometric and has infinite dimensions Moreover, a shape may have different representation or appearance due to translation, rotation, scaling and parametrization It is very desirable to find intrinsic characterization that are invariant under translation, rotation, scaling, and parametrization with certain robustness, especially with respect to noise In practice, it is necessary to characterize a shape using finite dimensional vectors that have the above desired properties In this dissertation, a novel method is proposed that uses the scattering relation and the response matrix This method has the advantage of robustness against noise and dealing with shape rotation and scaling The storage need for this method is small as well The details of our method on shape identification and classification will be discussed in Chapter 5

1 3 Research Objectives

The objective of this dissertation is to develop an iterative method for inverse scattering problem and to study the property of the response matrix, and the relation between the response matrix and the geometry of the target

In detail, research objectives of this dissertation include

1 To implement the forward solver for the forward scattering problem on Dirichlet and Neumann boundary condition using the Nystrom method,

2 To introduce the direct imaging method for inverse scattering problem,

3 To develop the iterative method for inverse scattering problem,

   (a) To convert the result of direct imaging method into the initial guess for the iterative method,

   (b) To solve forward problem and adjoint problem in each iteration,

4 To represent shapes using the response matrix and to study the application of response matrix in shape classification

1 4 Organization of the Dissertation

In Chapter 1, we will provide the general overview, research objectives, and organization of the dissertation

In Chapter 2, we will introduce the basic background of scattering theory and discuss the forward scattering problem, including the partial differential equation of the waves and numerical solution on $\mathbb{R}^2$ The forward solver will be implemented using Nystrom method and will be used in each iteration of the iterative method for inverse problem

In Chapter 3, we will introduce two direct imaging methods for inverse scattering problem the MUSIC method and the Multi-tone method Numerical results will be shown and will be used as the initial guess of the iterative method for inverse problem

In Chapter 4, we will develop the iterative method for the inverse scattering problem We will use active contour method to convert the image, which is the result of the direct imaging method, into level set function and capture the boundary of the target We will show that the result of adjoint problem will be the velocity vector of the sample points on the boundary We will solve one forward problem and one adjoint problem in each iteration We will show that the boundary converges to the real shape after several iterations

In Chapter 5, we will discuss the relation between response matrix and the geometry of the target We will define a distance function based on the response matrix to compare shapes We will study the property of the response matrix under different wave frequencies We will also apply our distance function on large data set to obtain the retrieval rate

In Chapter 6, we will provide a conclusion for this dissertation

CHAPTER 2

FORWARD PROBLEM

In this chapter, we will introduce the basic background of scattering theory and discuss the forward scattering problem, including the partial differential equation of the waves and numerical solution on $\mathbb{R}^2$ The forward solver will be implemented using Nystrom method for 2D scattering problem

2 1 Basic Conception

The target object is located in the center and is surrounded by an array of transducers, see Figure 2 1

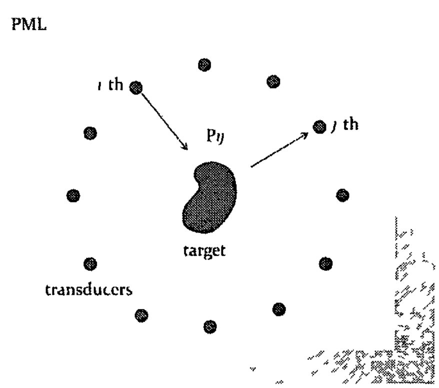

Figure 2 1 Generating the response matrix

Each transducer can emit acoustic/electromagnetic wave and receive scattered wave

Definition 2 1 1 The matrix $P = (P_{ij})_{N \times N}$ is called a **Response Matrix** if and only if P_{ij} is the received signal at j-th transducer for an incident plane wave sent from the i-th direction or an incident wave sent by the i-th transducer and N is the number of transducers

In general P may not be a square matrix There are two ways to obtain the response matrix P

1 Physical experiments and measurements

2 Numerical generations for solving the Helmholtz equation

In the iterative method for inverse scattering problem, we will solve the forward problem in each iteration step Therefore, the forward solver will be used on arbitrary shapes and the numerical solution is the only way to obtain the response matrix

2 2 The Helmholtz Equation

The Helmholtz Equation which governs the wave motion in forward solver is obtained from wave equation [12] Consider the propagation of sound waves of small amplitude in a homogeneous isotropic medium in $\mathbb{R}^3$ viewed as an inviscid fluid The wave motion is governed by Euler's equation

$$\frac{\partial v}{\partial t} + (v \;\; \nabla) v + \frac{1}{\rho} \nabla p = 0, \tag{2 1}$$

the equation of continuity

$$\frac{\partial \rho}{\partial t} + \nabla \;\; (\rho v) = 0, \tag{2 2}$$

the state equation

$$p = f(\rho, S), \tag{2 3}$$

and the adiabatic hypothesis

$$\frac{\partial S}{\partial t} + v \quad \nabla S = 0, \tag{2 4}$$

where $v = v(x,t)$ is the velocity field, $p = p(x,t)$ is the pressure, $\rho = \rho(x,t)$ is the density, $S = S(x,t)$ is the entropy, and f is a function depending on the nature of the fluid

For simplicity, the linearized Euler equation can be obtained by assuming that v, p, ρ and S are small perturbations of the static state $v_0 = 0$, $p_0 =$ constant, $\rho_0 =$ constant, $S_0 =$ constant

$$\frac{\partial v}{\partial t} + \frac{1}{\rho_0}\nabla p = 0, \tag{2 5}$$

the linearized equation of continuity

$$\frac{\partial \rho}{\partial t} + \rho_0 \nabla \quad v = 0, \tag{2 6}$$

the linearized state equation

$$\frac{\partial p}{\partial t} = \frac{\partial f}{\partial \rho}(\rho_0, S_0)\frac{\partial \rho}{\partial t} \tag{2 7}$$

From the linearized Equation (2 5)-(2 7) the wave equation is obtained

$$\frac{1}{c^2}\frac{\partial^2 f}{\partial t^2} = \triangle p, \tag{2 8}$$

where the speed of sound c is defined by

$$c^2 = \frac{\partial f}{\partial \rho}(\rho_0, S_0) \tag{2 9}$$

From the linearized Euler equation, it is observed that there exists a velocity potential $U = U(x,t)$ such that

$$v = \frac{1}{\rho_0}\nabla u, \tag{2 10}$$

and

$$p = -\frac{\partial U}{\partial t} \tag{2 11}$$

Clearly, the velocity potential also satisfied the wave equation

$$\frac{1}{c^2}\frac{\partial^2 U}{\partial t^2} = \triangle U \tag{2 12}$$

For time-harmonic acoustic waves of the form

$$U(x,t) = Re\{u(x)e^{-\imath\omega t}\}, \tag{2 13}$$

with frequency $\omega > 0$, the complex valued space dependent part u satisfies the Helmholtz equation

$$\triangle u + k^2 u = 0, \tag{2 14}$$

where the wave number k is given by the positive constant $k = \omega/c$

In obstacle scattering there are two cases of impenetrable and penetrable objects the sound-soft object and the sound-hard object For a sound-soft object, the pressure of the total wave vanishes on the boundary, and the total wave u satisfies the wave equation in the exterior $\mathbb{R}^3 \backslash \overline{D}$ of D with a Dirichlet boundary condition $u = 0$ on ∂D

Similarly, for a sound-hard object, the pressure satisfies the Neumann boundary condition $\partial u/\partial \nu = 0$ on ∂D where ν is the unit outward normal vector on the boundary ∂D The normal velocity of the total wave vanishes on the boundary

The solution of the Helmholtz equation (2 14) with positive wave number k can be deduced from the fundamental solution

$$\Phi(x,y) = \frac{1}{4\pi}\frac{e^{ik\|x-y\|}}{\|x-y\|},\ x \neq y \tag{2 15}$$

For a fixed $y \in \mathbb{R}^3$, the fundamental solution (2 15) satisfies the Helmholtz equation (2 14) in $\mathbb{R}^3 \backslash \{y\}$

The layer approach defines the single-layer and double-layer potentials

Definition 2 2 1 Acoustic Single-layer Potential Given any integral function φ, define the integral u such that

$$u(x) = \int_{\partial D} \varphi(y)\Phi(x,y)\mathrm{d}s(y), \tag{2 16}$$

where $\Phi(x,y)$ is the fundamental solution in (2 15) $u(x)$ is called the acoustic single-layer potential with density φ

Definition 2 2 2 Acoustic Double-layer Potential Given any integral function φ, define the integral v such that

$$v(x) = \int_{\partial D} \varphi(y)\frac{\partial\Phi(x,y)}{\partial\nu(y)}\mathrm{d}s(y), \tag{2 17}$$

where $\Phi(x,y)$ is the fundamental solution in Equation (2 15) $v(x)$ is called the acoustic double-layer potential with density φ

u and v are solutions to the Helmholtz equation (2 14) in D and in $\mathbb{R}^3 \backslash \overline{D}$ Any solution to the Helmholtz equation can be represented as a combination of single-layer and double-layer potentials

2 3 Scattering from an Obstacle

The scattering of time-harmonic acoustic waves by sound-soft obstacles leads to the following problems

Definition 2 3 1 Direct Acoustic Obstacle Scattering Problem Given an entire solution u^i to the Helmholtz equation representing an incident field, find a solution

$$u = u^i + u^s, \tag{2 18}$$

to the Helmholtz equation in $\mathbb{R}^3 \backslash \overline{D}$ such that the scattered field u^s satisfies the Sommerfeld radiation condition and the total field u satisfies the boundary condition

$$u = 0 \text{ on } \partial D \tag{2 19}$$

This direct scattering problem is a special case of the following Dirichlet problem

Definition 2 3 2 Exterior Dirichlet Problem Given a continuous function f on ∂D, find a radiating solution $u \in C^2(\mathbb{R}^3 \backslash \overline{D}) \bigcap C(\mathbb{R}^3 \backslash D)$ to the Helmholtz equation

$$\triangle u + k^2 u = 0 \text{ in } \mathbb{R}^3 \backslash \overline{D}, \tag{2 20}$$

which satisfies the boundary condition

$$u = f \text{ on } \partial D \tag{2 21}$$

The objective is to obtain the solution in the form of a combined acoustic single-layer and double-layer potentials, see [12]

The following theorem provides the solution of the Exterior Dirichlet Problem

Theorem 2 3 3 Define the potential $u(x)$ satisfying

$$u(x) = \int_{\partial D} \left\{ \frac{\partial \Phi(x,y)}{\partial \nu(y)} - i\eta \Phi(x,y) \right\} \varphi(y) \mathrm{d}s(y), \tag{2 22}$$

with a density $\varphi \in C(\partial D)$ and a real coupling parameter $\eta \neq 0$ Then the potential u given by Equation (2 22) in $\mathbb{R}^3 \backslash \overline{D}$ solves the Exterior Dirichlet Problem if and only if the density is a solution of the integral equation

$$\varphi + K\varphi - i\eta S\varphi = 2f, \tag{2.23}$$

where $S: C(\partial D) \to C(\partial D)$ is the single-layer operator defined by

$$(S\varphi)(x) = 2\int_{\partial D} \Phi(x,y)\varphi(y)\mathrm{d}s(y),\ x \in \partial D, \tag{2.24}$$

and $K: C(\partial D) \to C(\partial D)$ is the double-layer operator defined by

$$(K\varphi)(x) = 2\int_{\partial D} \frac{\partial\Phi(x,y)}{\partial\nu(y)}\varphi(y)\mathrm{d}s(y),\ x \in \partial D \tag{2.25}$$

The acoustic scattering from a sound-hard obstacle should follow the Exterior Neumann Problem

Definition 2.3.4 Exterior Neumann Problem Given a continuous function g on ∂D, find a radiating solution $u \in C^2(\mathbb{R}^3 \backslash \overline{D}) \bigcap C(\mathbb{R}^3 \backslash D)$ to the Helmholtz equation

$$\triangle u + k^2 u = 0 \text{ in } \mathbb{R}^3 \backslash \overline{D}, \tag{2.26}$$

which satisfies the boundary condition

$$\frac{\partial u}{\partial \nu} = g \text{ on } \partial D \tag{2.27}$$

Similarly, the following theorem provides the solution of the Exterior Neumann Problem

Theorem 2.3.5 Define the potential $u(x)$ satisfying

$$u(x) = \int_{\partial D} \left\{ \Phi(x,y)\varphi(y) + i\eta \frac{\partial\Phi(x,y)}{\partial\nu(y)}(S_0^2\varphi)(y) \right\} \mathrm{d}s(y), \tag{2.28}$$

with continuous density φ and a real coupling parameter $\eta \neq 0$. S_0 in Equation (2.28) denotes the single-layer operator S in Equation (2.24) in the potential theoretic limit case $k = 0$

Equation (2 28) solves the Exterior Neumann Problem if and only if the density is a solution of the integral equation

$$\varphi - K'\varphi - i\eta T S_0^2 \varphi = -2g, \tag{2 29}$$

where K' and T are the normal derivative operators given by

$$(K'\varphi)(x) \; = 2\int_{\partial D} \frac{\partial \Phi(x,y)}{\partial \nu(x)} \varphi(y) \mathrm{d}s(y), \;\; x \in \partial D, \tag{2 30}$$

and

$$(T\varphi)(x) \; = 2\frac{\partial}{\partial \nu(x)} \int_{\partial D} \frac{\partial \Phi(x,y)}{\partial \nu(y)} \varphi(y) \mathrm{d}s(y), \;\; x \in \partial D \tag{2 31}$$

2 4 Numerical Solution in $\mathbb{R}^2$

This section studies the numerical solution of the Helmholtz equation in $\mathbb{R}^2$ using the Nystrom method, which is based on appropriately weighted numerical quadratures on an equidistant mesh Therefore, the necessary parametrization of the integral equation in the two-dimensional case will be described It is assumed that the boundary curve ∂D possesses a regular analytic and 2π-periodic parametric representation of the form

$$x(t) = (x_1(t), x_2(t)), \qquad 0 \le t \le 2\pi, \tag{2 32}$$

in counterclockwise orientation satisfying $[x_1'(t)]^2 + [x_2'(t)]^2 > 0$ for all t

For the exterior Dirichlet problem, Equation (2 23) is transformed into the parametric form

$$\psi(t) - \int_0^{2\pi} \left[L(t,\tau) + i\eta M(t,\tau)\right] \psi(\tau) \mathrm{d}\tau = g(t), \;\; 0 \le t \le 2\pi, \tag{2 33}$$

where $\psi(t) = \varphi(x(t))$, $g(t) = 2f(x(t))$ and the kernels are given by

$$
\begin{aligned}
L(t,\tau) &= \frac{ik}{2}\left\{x_2'(\tau)\left[x_1(\tau)-x_1(t)\right]-x_1'(\tau)\left[x_2(\tau)-x_2(t)\right]\right\}\frac{H_1^{(1)}(kr(t,\tau))}{r(t,\tau)}, && (2.34)\\
M(t,\tau) &= \frac{i}{2}H_0^{(1)}(kr(t,\tau))\left\{[x_1'(\tau)]^2+[x_2'(\tau)]^2\right\}^{1/2}, && (2.35)
\end{aligned}
$$

for $t \neq \tau$ Here, let

$$
r(t,\tau) = \left\{[x_1(t)-x_1(\tau)]^2+[x_2(t)-x_2(\tau)]^2\right\}^{1/2} \tag{2.36}
$$

Note that the kernels L and M have logarithmic singularities at $t=\tau$ Hence, using the numerical method introduced in [26], the kernels are split into

$$
\begin{aligned}
L(t,\tau) &= L_1(t,\tau)\ln\left(4\sin^2\frac{t-\tau}{2}\right)+L_2(t,\tau), && (2.37)\\
M(t,\tau) &= M_1(t,\tau)\ln\left(4\sin^2\frac{t-\tau}{2}\right)+M_2(t,\tau), && (2.38)
\end{aligned}
$$

where

$$
\begin{aligned}
L_1(t,\tau) &= \frac{k}{2\pi}\left\{x_2'(\tau)\left[x_1(t)-x_1(\tau)\right]-x_1'(\tau)\left[x_2(t)-x_2(\tau)\right]\right\}\frac{J_1(kr(t,\tau))}{r(t,\tau)}, && (2.39)\\
L_2(t,\tau) &= L(t,\tau)-L_1(t,\tau)\ln\left(4\sin^2\frac{t-\tau}{2}\right), && (2.40)\\
M_1(t,\tau) &= -\frac{1}{2\pi}J_0(kr(t,\tau))\left\{[x_1'(\tau)]^2+[x_2'(\tau)]^2\right\}^{1/2}, && (2.41)\\
M_2(t,\tau) &= M(t,\tau)-M_1(t,\tau)\ln\left(4\sin^2\frac{t-\tau}{2}\right) && (2.42)
\end{aligned}
$$

The kernels L_1, L_2, M_1, and M_2 turn out to be analytic

In particular, for the $t=\tau$ terms, there are

$$
L_2(t,t) = L(t,t) = \frac{1}{2\pi}\frac{x_1'(t)x_2''(t)-x_2'(t)x_1''(t)}{[x_1'(t)]^2+[x_2'(t)]^2}, \tag{2.43}
$$

and

$$
M_2(t,t) = \left\{\frac{i}{2}-\frac{C}{\pi}-\frac{1}{2\pi}\ln\left(\frac{k^2}{4}\{[x_1'(t)]^2+[x_2'(t)]^2\}\right)\right\}\left\{[x_1'(t)]^2+[x_2'(t)]^2\right\}^{1/2}, \tag{2.44}
$$

for $0 \le t \le 2\pi$

Hence, it is necessary to numerically solve the integral equation of the form

$$\varphi(t) - \int_0^{2\pi} K(t,\tau)\varphi(\tau)\mathrm{d}\tau = g(t), \qquad 0 \le t \le 2\pi, \tag{2 45}$$

where the kernel K can be written as

$$K(t,\tau) = K_1(t,\tau)\ln\left(4\sin^2\frac{t-\tau}{2}\right) + K_2(t,\tau), \tag{2 46}$$

with analytic functions K_1 and K_2 and with an analytic right hand side g

Here it is necessary to point out that it is essential to split off the logarithmic singularity in a fashion which preserves the 2π-periodicity for the kernels K_1 and K_2 This treatment guarantees the exponential convergence of the numerical solution, which will be demonstrated in the numerical experiments

The Nystrom method uses a straightforward approximation of the integrals by quadrature formulas In this case, since the boundary of the target ∂D is a 2π-periodic form, an equidistant set of knots $t_j = \pi j/n$, $j = 0, \quad , 2n-1$ were chosen, and use the quadrature rule

$$\int_0^{2\pi} \ln\left(4\sin^2\frac{t-\tau}{2}\right) f(\tau)\mathrm{d}\tau \approx \sum_{j=1}^{2n-1} R_j^{(n)}(t) f(t_j), \qquad 0 \le t \le 2\pi, \tag{2 47}$$

with the quadrature weights given by

$$R_j^{(n)}(t) = -\frac{2\pi}{n}\sum_{m=1}^{n-1}\frac{1}{m}\cos m(t-t_j) - \frac{\pi}{n^2}\cos n(t-t_j), \qquad j = 0, \quad , 2n-1, \tag{2 48}$$

and the trapezoidal rule

$$\int_0^{2\pi} f(\tau)\mathrm{d}\tau \approx \frac{\pi}{n}\sum_{j=0}^{2n-1} f(t_j), \tag{2 49}$$

where the function f can represent any integration kernel The numerical integrations are obtained from integrating exactly

In the Nystrom method, the integral in Equation (2 45) is replaced by the finite summation, and yields

$$\psi^{(n)}(t) - \sum_{j=0}^{2n-1} \left\{ R_j^{(n)}(t) K_1(t, t_j) + \frac{\pi}{n} K_2(t, t_j) \right\} \psi^{(n)}(t_j) = g(t), \qquad (2\ 50)$$

for $0 \leq t \leq 2\pi$

Equation (2 50) is obtained from Equation (2 45) by applying the quadrature rule, Equation (2 47), to $f = K_1(t, \ )\psi$, and trapezoidal rule, Equation (2 49), to $f = K_2(t, \ )\psi$ The solution of Equation (2 50) reduces to solving a finite dimensional linear system

In particular, for any solution of Equation (2 50) the values

$$\psi_i^{(n)} = \psi^{(n)}(t_i), \qquad i = 0, \quad , 2n-1, \qquad (2\ 51)$$

satisfy the linear system

$$\psi_i^{(n)} - \sum_{j=0}^{2n-1} \left\{ R_{|i-j|}^{(n)} K_1(t_i, t_j) + \frac{\pi}{n} K_2(t_i, t_j) \right\} \psi_j^{(n)} = g(t_i), \qquad (2\ 52)$$

for $i = 0, \quad , 2n-1$, where

$$R_j^{(n)} = R_j^{(n)}(0) = -\frac{2\pi}{n} \sum_{m=1}^{n-1} \frac{1}{m} \cos \frac{mj\pi}{n} - \frac{(-1)^j \pi}{n^2}, \qquad j = 0, \quad , 2n-1 \qquad (2\ 53)$$

Conversely, given a solution $\psi_i^{(n)}$, $i = 0, \quad , 2n-1$ of the linear system of Equation (2 52), the function $\psi^{(n)}$ defined by

$$\psi^{(n)}(t) = \sum_{j=0}^{2n-1} \left\{ R_j^{(n)}(t) K_1(t, t_j) + \frac{\pi}{n} K_2(t, t_j) \right\} \psi^{(n)}(t_j) + g(t), \qquad (2\ 54)$$

for $0 \leq t \leq 2\pi$ satisfies the approximating Equation (2 50)

Once the density function ψ is obtained, the total field u can be determined using Theorem 2 3 3 since ψ is the discrete form of φ

The Nystrom method for Neumann boundary condition is similar to but more complicated than the Dirichlet boundary condition [27] The Exterior Neumann Problem solver will be used in the adjoint problem in the iterative method of inverse problem

2 5 Numerical Experiments

The forward solvers for Exterior Dirichlet problem and Exterior Neumann problem are implemented First place four transducers around the target, which is a flower shape in Figure 2 2

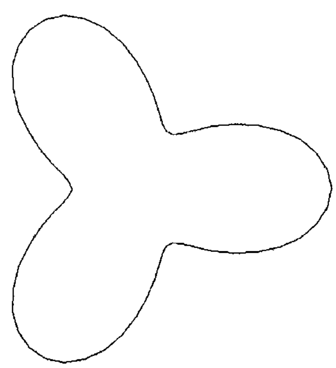

Figure 2 2 Flower shape

The flower shape has following analytic presentation

$$x(t) = (1 + 0\ 5\cos(3t)) * \cos(t), \tag{2 55}$$

and

$$y(t) = (1 + 0\ 5\cos(3t)) * \sin(t) \tag{2 56}$$

The location of four transducers are $l_1 = (5, 0)$, $l_2 = (0, 5)$, $l_3 = (-5, 0)$, and $l_4 = (0, -5)$ Let n be the number of sample points on the boundary of the target, and k be the wave number The response matrix generated by Exterior Dirichlet forward solver at $k = 1$, $n = 64$ is

$$P = \begin{pmatrix} -0\ 093 + 0\ 198i & -0\ 084 + 0\ 194i & -0\ 075 + 0\ 189i & -0\ 084 + 0\ 194i \\ -0\ 084 + 0\ 194i & -0\ 093 + 0\ 198i & -0\ 084 + 0\ 194i & -0\ 075 + 0\ 190i \\ -0\ 075 + 0\ 190i & -0\ 084 + 0\ 194i & -0\ 093 + 0\ 198i & -0\ 084 + 0\ 194i \\ -0\ 084 + 0\ 194i & -0\ 075 + 0\ 190i & -0\ 084 + 0\ 194i & -0\ 093 + 0\ 198i \end{pmatrix} \qquad (2\ 57)$$

If the scatter field incident from l_1 and received by l_2 is taken, and consider the change of n, the $P_{2,1}$ term of response matrix P will be

$$n = 16, \qquad P_{2,1} = -0\ 084642954035770 + 0\ 193994448938375i,$$

$$n = 32, \qquad P_{2,1} = -0\ 084642528632574 + 0\ 194003759720873i,$$

$$n = 64, \qquad P_{2,1} = -0\ 084642633363342 + 0\ 194003674480984i,$$

$$n = 128, \qquad P_{2,1} = -0\ 084642633328078 + 0\ 194003674511525i,$$

$$n = 256, \qquad P_{2,1} = -0\ 084642633328085 + 0\ 194003674511490i$$

Numerical result shows that the forward solver converges with the number of sample points on the target boundary Figure 2 3 shows the convergence rate

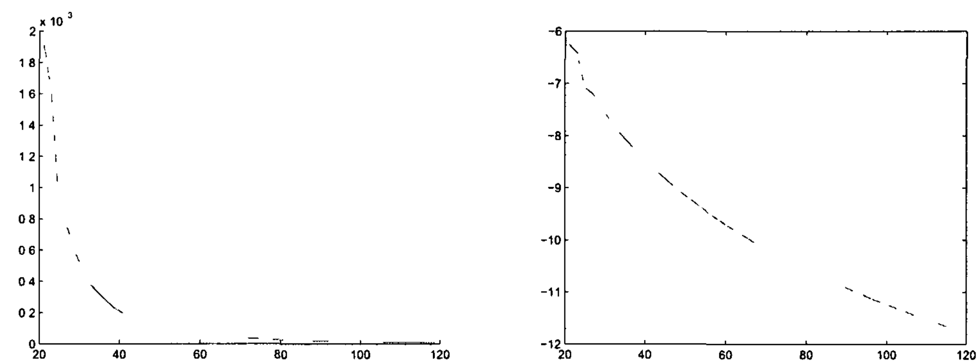

Figure 2 3 Convergence of the Nystrom method

In Figure 2 3, $P^{(320)}$ is used to approximate the real response matrix at $n = 320$, and consider the error $err^{(n)}$ such that

$$err^{(n)} = \max_{1 \leq i \leq 4, 1 \leq j \leq 4} |P_{i,j}^{(n)} - P_{i,j}^{(320)}| \tag{2 58}$$

The left picture in Figure 2 3 is $err^{(n)}$, the right one is $\log(err^{(n)})$, and here n goes from 20 to 120 From Figure 2 3 it can be seen that the result of the Nystrom method has the exponential convergence

$$err^{(n)} \leq Ce^{-\sigma n} \tag{2 59}$$

For this example, if $C \approx 3\ 4 \times 10^{-4}$ and $\sigma \approx 0\ 03$, the Equation (2 59) holds for large enough n

The Nystrom method can be also applied on multiple arbitrary targets In Figure 2 4, two targets are placed in the domain

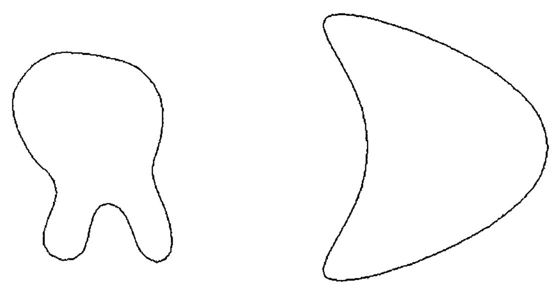

Figure 2 4 Two arbitrary shapes

The number sample points on the left target, n_1, is twice as the right one, n_2, since the left one is more complicated in the geometry than the right one The far field pattern is used this time, 4 transducers are place at infinity so the coming wave can be viewed as a plain wave, and $P_{4,2}$ term has the following result

$$n_1 = 20,\ n_2 = 10,\ P_{4,2} = 0\ 861545181700902 + 0\ 768278897453679\imath,$$

$$n_1 = 40,\ n_2 = 20,\ P_{4,2} = 0\ 558175744822589 + 0\ 326216480242953\imath,$$

$$n_1 = 80,\ n_2 = 40,\ P_{4,2} = 0\ 598846321309680 + 0\ 344732099974921\imath,$$

$$n_1 = 160,\ n_2 = 80,\ P_{4,2} = 0\ 603846677808666 + 0\ 343570140247151\imath,$$

$$n_1 = 320,\ n_2 = 160,\ P_{4,2} = 0\ 606402604809483 + 0\ 342939623306911\imath$$

The response matrix also converges when $n_1 \to \infty$ and $n_2 \to \infty$

2 6 Summary for Forward Solver

The forward solver presented in this chapter will be used in the iterative method for inverse problem The Nystrom method is used to obtain the scattered field The Nystrom method requires the least computational effort comparing to the Galerkin method, since only two one-dimensional integral equations needed to be computed The error between numerical result and the real data converges exponentially with respect to the number of sample points on the boundary of the target Each column of the response matrix is the scattered field coming from one transducer Every column is independent of each other in the response matrix Therefore, when the number of transducers is large, the forward solver can be parallelized easily each processor deals with the wave coming from one transducer and computes one column of the response matrix

CHAPTER 3

DIRECT METHOD FOR INVERSE PROBLEM

In this chapter, two direct imaging methods will be introduced The MUSIC method is a projection method that can be applied on full aperture, the Multi-tone method utilizes the phase information of the response matrix and multi-frequency wave that can be applied on limited or synthetic aperture

3 1 Introduction of Inverse Problem

Recall the definition of the **Response Matrix** $P = \{P_{ij}\}_{N\times N}$, where P_{ij} is the received signal at j-th transducer for an incident plane wave sent from the i-th direction and N is the number of transducers In general P may not be a square matrix

The medium properties will be probed from a scattered wave field The time harmonic wave field $u(x)$ satisfies

$$\Delta u(x) + k^2 n(x) u = f(x), \tag{3 1}$$

where k is the wave number, $n(x)$ is the index of refraction, and $f(x)$ is the source

The general inverse problem is to find $n(x)$ inside the interested region If $n(x)$ is piecewise constant, the objective is simplified to find the boundaries where $n(x)$ jumps Therefore, the inverse scattering problem is reduced to determine the boundary of a target The inverse problem is widely used in industry, such as in medical imaging, underwater acoustics, and non-destructive detection

3 2 Property of the Response Matrix

Let L be the distance between the transducer and the target, a be the length of the array of transducers Figure 3 1 shows the full aperture and limited/synthetic aperture

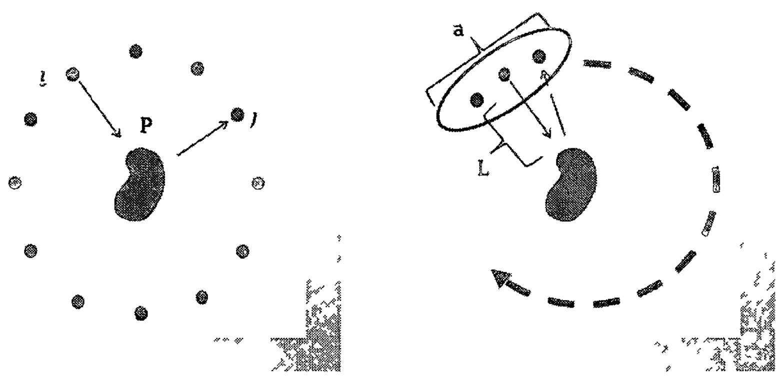

Figure 3 1 Full aperture and limited/synthetic aperture

Define R to be the resolution of the array

$$R = \frac{\lambda L}{a}, \tag{3 2}$$

where

$$\lambda = \frac{2\pi}{k} \tag{3 3}$$

Let S be the size of the target There are three different cases

1 **Point target** ($S \ll R$)

(a) The rank of the response matrix is equal to the number of targets

(b) Only location information of the targets can be recovered

(c) The singular values of the response matrix is shown in the left picture of Figure 3 2

2 **Small target** ($S < R$)

(a) The response matrix has a discrete spectrum

(b) Both location and size (moment) information of the targets can be recovered

(c) The response matrix has grouped singular values, see the middle picture of Figure 3 3

3 **Extended target** ($S \geq R$)

(a) The response matrix has a continuous spectrum

(b) Both location and geometry information of the targets can be recovered

(c) The number of significant singular values and singular vectors of the response matrix is $\propto S/R$, see the right picture of Figure 3 4

This chapter focuses on the third case since the objective is to reconstruct the shape of the target The wave number k should be large enough to capture the shape information of the target

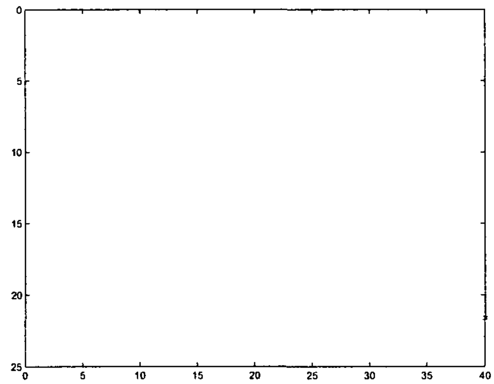

Figure 3 2 Resolution v s target size Point target

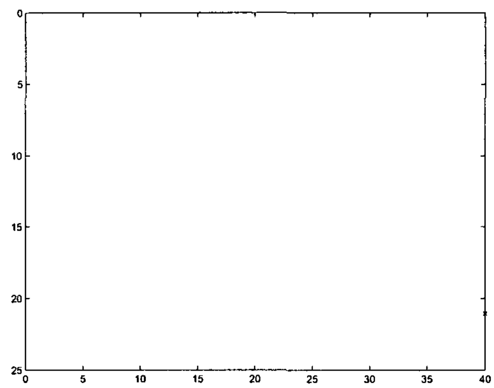

Figure 3 3 Resolution v s target size Small target

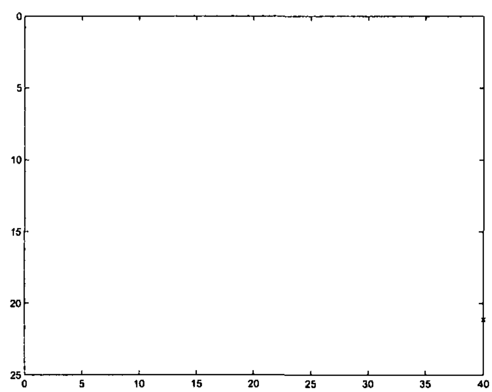

Figure 3 4 Resolution v s target size Extended target

3 3 The MUSIC (MUltiple SIgnal Classification) Algorithm

The MUltiple SIgnal Classification (MUSIC) method is one of the direct imaging methods There are several advantages to the MUSIC method

1 No iteration or forward problem solver is needed

2 This method works for both near field and far field data

3 Material property can be embedded into the imaging function

4 Resolution based thresholding is quite robust with noise

The MUSIC method for point target and small target is discussed in [15] For the extended target of Dirichlet boundary condition, let Ω denote the target The scattered field u^s satisfies

$$\begin{cases} \Delta u^s(x) + k^2 u^s(x) = 0 & x \in \Omega^c \subset R^d \\ u^s(x) = -u^i(x) & x \in \partial\Omega \end{cases}, \tag{3 4}$$

and the Sommerfeld Radiation Condition (1 5), where u^i is the incident field

Let $G_D(x,y)$ be the Green's function that satisfies

$$\begin{cases} \Delta G_D(x) + k^2 G_D(x) = \delta(x-y) & x, y \in \Omega^c \subset R^d \\ G_D(x,y) = 0 & x \in \partial\Omega \end{cases}, \tag{3 5}$$

and the Sommerfeld Radiation Condition (1 5)

Hence, the scattered field u^s can be written as

$$u^s(x) = \int_{\partial\Omega} u^i(y) \frac{\partial G_D(x,y)}{\partial \nu} dy \tag{3 6}$$

The scattered field u^s is factorized into two parts

1 Unknown part the Green's function $G_D(x,y)$ which depends on the shape of the unknown target

2 Known part u^i is the illumination wave field that can be controlled

The key point to determine the boundary of the target is to define the illumination vector and signal space

Definition 3 3 1 Illumination Vector Let $G_0(\ ,\ )$ and $G_D(\ ,\ )$ be the homogeneous and inhomogeneous Green's function, respectively Define

$$\vec{g}_0(x) = [G_0(x_1, x), G_0(x_2, x), \quad , G_0(x_N, x)]^T, \tag{3 7}$$

$$\vec{g}_D(x) = [G_D(x_1, x), G_D(x_2, x), \quad , G_D(x_N, x)]^T, \tag{3 8}$$

where $x_1, x_2, \quad , x_N$ are the locations of N transducers Then $\vec{g}_0(x)$ and $\vec{g}_D(x)$ are called the illumination vectors

If a point source wave is emitted at i-th transducer and the scattered field is received by the j-th transducer, the P_{ij} term of the response matrix is

$$P_{ij} = \int_{\partial\Omega} \frac{\partial G_D(x_j, y)}{\partial \nu} G_0(x_i, y) dy \tag{3 9}$$

In matrix form the response matrix can be factorized as

$$P = \int_{\partial\Omega} \vec{g}_0(y) \left[\frac{\partial \vec{g}_D(y)}{\partial \nu} \right]^T dy \tag{3 10}$$

Definition 3 3 2 Signal Space Let $\vec{u}_i$ be the singular vectors with singular values σ_i of the response matrix P Define the signal space

$$V_s = span\{\vec{u}_i | i \leq n\}, \tag{3 11}$$

where n is a threshold depending on the resolution of the array and the noise level

The threshold parameter n in Equation (3 11) can be determined using the resolution analysis which is introduced in [18]

Then the imaging function I^M can be defined as

$$I^M(x) = \|(I - P_{V_S})\vec{g}_0(x)\|^{-1}, \tag{3 12}$$

where P_{V_S} is a projection operator projecting the homogeneous illumination vector $\vec{g}_0(x)$ into the signal space

Then, when x get close to the boundary ∂D, $\vec{g}_0(x)$ should be in signal space The $I - P_{V_S}$ is a projection operator which project the illumination vector into the noise space Therefore, $(I - P_{V_S})\vec{g}_0(x)$ should be small when x goes to ∂D, and $I^M(x)$ will peak at the boundary

The MUSIC method is a direct approach for the inverse scattering problem It is efficient and robust since no inverse operation or iteration is needed

3 4 Examples for MUSIC method

The MUSIC method can be applied on single or multiple targets with Dirichlet Boundary Condition, see Figure 3 5

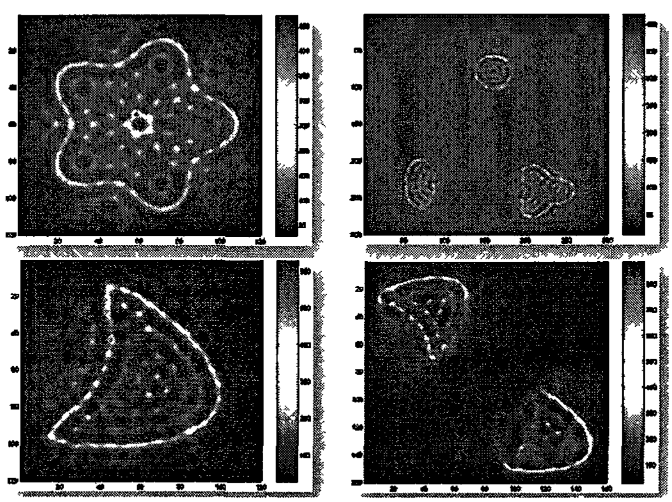

Figure 3 5 Imaging extended target with Dirichlet BC

More results of MUSIC method on an extended target can be found in [18] The image of MUSIC method provides a rough picture of the geometry of the target Chapter 4 will show how to start with the image of MUSIC method and use the iterative method to obtain more accurate results

3 5 Direct Imaging Method using Multi-frequency Data

The MUSIC method uses a single frequency and cannot be applied on limited or synthetic aperture The MUSIC method is essentially a projection method which drops the phase information when projecting to the signal space Using the multi-frequency data and phase information, provides better results for limited or synthetic data

For the limited or synthetic aperture, there are two cases

1 The emitters and receivers coincide

2 The emitters and receivers do not coincide

In the first case, the response matrix P is complex symmetric Then P can be written as $P = U\Sigma U^T$ This unique factorization (up to a sign) helps to eliminate the arbitrary phase generated by MATLAB when taking the singular value decomposition The imaging function is defined as

$$I^M(x) = \sum_{\omega} \alpha(\omega) \sum_{m=1}^{M^\omega} [\hat{g}^H(x,\omega) u_m^\omega]^2, \tag{3 13}$$

where $\hat{g}$ is the normalized illumination vector from the transducers to a search point x, u_m is the m-th row of the matrix U, α is the weight for multi-spectrum, M^ω is a threshold

In the second case, suppose that there are s transmitters located at $\xi_1, \quad , \xi_s$ and there are r receivers located at $\eta_1, \quad , \eta_r$, the response matrix P has the dimension

$s \times r$ P_{ij} records the signal received by the j-th receiver at η_j when the wave comes from the i-th emitter at ξ_i

At this time the illumination vectors need to be redefined with respect to the receiver array and emitter array, respectively, as

$$g_r(x) = [G_0(\eta_1, x), G_0(\eta_2, x), \quad , G_0(\eta_r, x)]^T, \tag{3 14}$$

and

$$g_s(x) = [G_0(\xi_1, x), G_0(\xi_2, x), \quad , G_0(\xi_s, x)]^T \tag{3 15}$$

Then the imaging function is

$$I^M(x) = \sum_{\omega} \alpha(\omega) \sum_{m=1}^{M^{\omega}} [\hat{g}_r^H(x,\omega) u_m^{\omega}][\hat{g}_s^H(x,\omega) \overline{v}_m^{\omega}] \tag{3 16}$$

When providing limite/synthetic aperture, Figure 3 6 shows that good results can still be obtained using Multi-frequency method

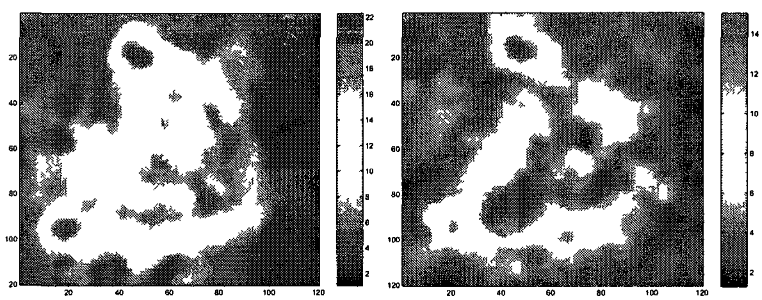

Figure 3 6 Multi-tone method on synthetic aperture

In Figure 3 6, the left image is imaging using synthetic aperture data with 10% multiplicative noise, the right one is imaging using synthetic aperture data in a weakly inhomogeneous medium More results of Multi-tone method can be found in [16]

3 6 Summary for Dırect Imagıng

The dırect ımagıng method ıs computatıonally effıcıent compared to the ıteratıve method The MUSIC and Multı-frequency methods both work for near field and far field data, and can ıncorporate materıal propertıes (correspondıng to dıfferent boundary condıtıons) Sınce each of the two methods apply thresholdıng based on SVD and physıcal scales, the results are robust wıth respect to noısy data Furthermore, Multı-frequency data can be used to obtaın an ıdeal result under lımıted or synthetıc aperture

CHAPTER 4

ITERATIVE METHOD FOR INVERSE PROBLEM

In this chapter, we will develop the iterative method for the inverse scattering problem The main idea is to an optimization problem Similar approach is used in [17] and [2] We will use active contour method to convert the image, which is the result of the direct imaging method, into level set function and capture the boundary of the target We will show that the result of adjoint problem will be the velocity vector of the sample points on the boundary We will solve one forward problem and one adjoint problem in each iteration Finally, we will demonstrate that the boundary converges to the real shape after several iterations

4 1 Image Processing and the Level Set Representation

The result of the direct imaging method is used as the initial guess of the iterative method The output of direct imaging method is an image of the whole domain and the value peak at the boundary of the object The first thing needs to be done is to locate the boundary from the image and transform it into parameter representation which can be used as the input of the forward problem

The gradient flow method and active contour method can both be used to capture convex envelope of the boundary of the object The main idea is to transform the image into a level set function The gradient flow method is outlined as follows

1 Input the MUSIC imaging function $I(x)$

2 Apply a threshold to the MUSIC imaging function

3 Consider the cost functional to be minimized

$$C(\partial\Omega) = \int_{\partial\Omega} f(x)ds, \tag{4 1}$$

where

$$f(x) = \begin{cases} 1, & I(x) > M \\ 100, & I(x) \leq M \end{cases}, \tag{4 2}$$

and $I(x)$ is the image function, M is the constant representing the threshold

4 Rewrite the cost functional using the level set representation

$$C(\partial\Omega) = W(\phi) = \int_{R^2} f(x)\delta(\phi) \mid \nabla\phi \mid dx \tag{4 3}$$

5 Take derivative with respect to the evolution time t and derive the gradient flow equation

$$\phi_t = \mid \nabla\phi \mid \nabla \left(f(x)\frac{\nabla\phi}{\mid \nabla\phi \mid} \right) \tag{4 4}$$

6 Calculate the level set representation for the initial guess

The method above is simple and easy to implement The drawback is that it can only capture the convex envelop

The software motivated by the active contour method [6] and developed for [35] is used here to generate the level set function representing the object

The forward solver using the Nystrom method for the obstacle problem with Dirichlet boundary condition needs not only the coordinates of the sample points $(x(t_i), y(t_i))$ but also the first and second derivatives $(x'(t_i), y'(t_i)), (x''(t_i), y''(t_i))$

Trigonometric interpolation is used to convert a set of sample points to a pair of analytic functions $(x(t), y(t))$

$$x(t) = \sum_{n=1}^{N} (a_n \cos(nt) + b_n \sin(nt)), \tag{4 5}$$

$$y(t) = \sum_{n=1}^{N} (c_n \cos(nt) + d_n \sin(nt)), \tag{4 6}$$

where the coefficients $\{a_n\}_{n=1}^{N}$, $\{b_n\}_{n=1}^{N}$, $\{c_n\}_{n=1}^{N}$, $\{d_n\}_{n=1}^{N}$ are determined by the sample points $\{(x(t_i), y(t_i))\}_{n=1}^{m}$ separately to achieve the least square distance

Note that the order of the interpolation N should be less than $m/2$ The dummy parameter d is generated to be equally distributed between 0 and 2π by $d_i = 2\pi i/m$, $i = 0, 1, \quad , m-1$, and define matrix A such that

$$A_{2j,2k} = \sum_{i=0}^{m-1} \cos(jd_i) \cos(kd_i), \tag{4 7}$$

$$A_{2j+1,2k+1} = \sum_{i=0}^{m-1} \sin(jd_i) \sin(kd_i), \tag{4 8}$$

$$A_{2j,2k+1} = \sum_{i=0}^{m-1} \cos(jd_i) \sin(kd_i), \tag{4 9}$$

$$A_{2j+1,2k} = \sum_{i=0}^{m-1} \sin(jd_i) \cos(kd_i) \tag{4 10}$$

$$A_{1,2j} = A_{2j,1} = \sum_{i=0}^{m-1} \cos(jd_i), \tag{4 11}$$

$$A_{1,2j+1} = A_{2j+1,1} = \sum_{i=0}^{m-1} \sin(jd_i), \tag{4 12}$$

for $j, k = 1, 2, \quad , m$, and vector b_x, b_y such that

$$b_{2j} = \sum_{i=0}^{m-1} \cos(jd_i), \tag{4 13}$$

$$b_{2j+1} = \sum_{i=0}^{m-1} \sin(jd_i) \tag{4 14}$$

The interpolation coefficients $\{a_n\}_{n=1}^N$, $\{b_n\}_{n=1}^N$, $\{c_n\}_{n=1}^N$, $\{d_n\}_{n=1}^N$ can be obtained from A and b

Then, the boundary of the shape is re-sampled after each iteration and the first and second derivatives can be easily obtained

4 2 Recursive Linearization

The iterative method starts from the initial guess with initial wave number k_0 Suppose that after several iterations the boundary $\Gamma_{\tilde{k}}$ has been recovered at some wave number $\tilde{k}$ using the forward solver in Chapter 2, and that the next step wave number is k such that $k > \tilde{k}$ The objective is to determine Γ_k,

$$\Gamma_k = \{x + a(x) \quad x \in \Gamma_{\tilde{k}}\} \tag{4 15}$$

Here the new boundary Γ_k can be viewed as an updating from the boundary $\Gamma_{\tilde{k}}$ on previous step Since $\Gamma_{\tilde{k}}$ is know, the objective is to determine the perturbation a, which is also called the velocity vector of the sample points on the boundary

The reconstructed boundary $\Gamma_{\tilde{k}}$ is solved at the wave number k from the forward scattering problem

$$\begin{aligned} \Delta\tilde{u} + k^2\tilde{u} &= 0 \text{ in } \Omega^e_{\tilde{k}}, && (4\ 16) \\ \tilde{u} &= 0 \text{ on } \Gamma_{\tilde{k}}, && (4\ 17) \end{aligned}$$

with a scattered field satisfying the Sommerfeld Radiation Condition (1 5)

For the boundary Ω_k, there is

$$\begin{aligned} \Delta u + k^2 u &= 0 \text{ in } \Omega^e_k, && (4\ 18) \\ u &= 0 \text{ on } \Gamma_k && (4\ 19) \end{aligned}$$

Given a solution u in Equation (4 18), the corresponding scattered field u^s can be obtained and the measurement $\mathcal{M}$ can be defined

$$\mathcal{M}u^s(x) = [u^s(\mathbf{x}_1), \quad , u^s(\mathbf{x}_m)]^T, \tag{4 20}$$

where the operator $\mathcal{M}$ maps the scattered fields to a vector of complex numbers in $\mathbb{C}^m$

For the boundary Γ_k, the forward scattering operator is defined

$$\mathcal{F}(\Gamma_k) = \mathcal{M}u^s \tag{4 21}$$

Now the Fréchet derivative of $\mathcal{F}$ at $\Gamma_{\tilde{k}}$ is $\mathcal{F}'(\Gamma_{\tilde{k}})$ which satisfies

$$\mathcal{F}(\Gamma_k) = \mathcal{F}(\Gamma_{\tilde{k}}) + \mathcal{F}'(\Gamma_{\tilde{k}})a + o(\|a\|_{1,\infty}) \text{ as } \|a\|_{1,\infty} \to 0, \tag{4 22}$$

where $\|a\|_{1,\infty} = \max_{x\in\Gamma} |a(x)| + \max_{x\in\Gamma} \sum_{j=1}^{2} |\nabla a_j(x)|$ with surface gradient $\nabla a_j(x)$ of the j-th component of a The Fréchet derivative of the forward scattering operator is given by Theorem 2 1 in [23]

In order to compute the velocity vector a, the following theorem is needed

Theorem 4 2 1 Let $\Gamma_{\tilde{k}} \in C^2$, $a \in C^2(\Gamma_{\tilde{k}}, \mathbb{R}^2)$ and $\tilde{u}$ be the solution of the scattering problem in Equation (4 16)-(4 17) Then the Fréchet derivative of $\mathcal{F}(\Gamma_{\tilde{k}})$ satisfies $\mathcal{F}'(\Gamma_{\tilde{k}})a = \mathcal{M}v$, where v solves the following boundary value problem

$$\Delta v + k^2 v = 0 \text{ in } \Omega^e_{\tilde{k}}, \tag{4 23}$$

$$v = -a \quad n\frac{\partial \tilde{u}}{\partial n} \text{ on } \Gamma_{\tilde{k}}, \tag{4 24}$$

with radiation condition, where n is the unit outward normal vector on $\Gamma_{\tilde{k}}$

Denote the residual operator as

$$\mathcal{R}(\Gamma_{\tilde{k}}) = \mathcal{M}u^s - \mathcal{F}(\Gamma_{\tilde{k}}) \tag{4 25}$$

The lınearızed versıon of Equatıon (4 21) ıt ıs obtaıned such that

$$\mathcal{F}'(\Gamma_{\tilde{k}})a = \mathcal{R}(\Gamma_{\tilde{k}}) \tag{4 26}$$

Applyıng the Landweber ıteratıon to the lınearızed equatıon (4 26) yıelds

$$a = \beta\mathcal{F}'(\Gamma_{\tilde{k}})^*\mathcal{R}(\Gamma_{\tilde{k}}), \tag{4 27}$$

where $\mathcal{F}'(\Gamma_{\tilde{k}})^*$ ıs the adjoınt operator of $\mathcal{F}'(\Gamma_{\tilde{k}})$ and β ıs a posıtıve relaxatıon parameter

Sınce a depends on $\mathcal{F}'(\Gamma_{\tilde{k}})^*\mathcal{R}(\Gamma_{\tilde{k}})$ by Equatıon (4 27), ıt ıs necessary to find the value of $\mathcal{F}'(\Gamma_{\tilde{k}})^*\mathcal{R}(\Gamma_{\tilde{k}})$ However, ıt ıs dıfficult to compute $\mathcal{F}'(\Gamma_{\tilde{k}})^*\mathcal{R}(\Gamma_{\tilde{k}})$ dırectly The adjoınt problem ıs ıntroduced to solve thıs problem

Let $\mathcal{R}(\Gamma_{\tilde{k}}) = [\xi_1, \quad , \xi_m]^T \in \mathbb{C}^m$ Consıder the adjoınt problem

$$\Delta w + k^2 w = -\sum_{j=1}^{m} \xi_j \delta(x - x_j) \text{ in } \Omega^e_{\tilde{k}}, \tag{4 28}$$

$$w = 0 \text{ on } \Gamma_{\tilde{k}}, \tag{4 29}$$

wıth the Sommerfeld Radıatıon Condıtıon (1 5)

Multıplyıng $\bar{w}$ to the Equatıon (4 23) and ıntegratıng over $\Omega^e_{\tilde{k}}$ on both sıdes yıelds the followıng result

$$\int_{\Omega^e_{\tilde{k}}} (\Delta v + k^2 v)\bar{w} \mathrm{d}x = 0, \tag{4 30}$$

where $\bar{w}$ ıs the complex conjugate of w

Usıng the Green's formula, there ıs

$$\int_{\Omega^e_{\tilde{k}}} (\Delta\bar{w} + k^2\bar{w})v \mathrm{d}x = \int_{\Gamma_{\tilde{k}}} \left(\frac{\partial v}{\partial n}\bar{w} - \frac{\partial \bar{w}}{\partial n}v\right) \mathrm{d}s \tag{4 31}$$

It follows from the adjoınt equatıon (4 28) and the boundary condıtıon (4 24) that

$$\sum_{j=1}^{m} v(x_j)\bar{\xi}_j = -\int_{\Gamma_{\tilde{k}}} \frac{\partial \bar{w}}{\partial n}\frac{\partial u}{\partial n} a \quad n \mathrm{d}s \tag{4 32}$$

Noting Equation (4 20), Equation (4 25), and Theorem 4 1, the left-hand side of Equation (4 32) can be reduced

$$\begin{aligned}\sum_{j=1}^{m} v(x_j)\bar{\xi}_j &= < \mathcal{M}v, \mathcal{R}(\Gamma_{\tilde{k}}) >_{\mathbb{C}^m} \\ &= < \mathcal{F}'(\Gamma_{\tilde{k}})a, \mathcal{R}(\Gamma_{\tilde{k}}) >_{\mathbb{C}^m} \\ &= < a, \mathcal{F}'(\Gamma_{\tilde{k}})^*\mathcal{R}(\Gamma_{\tilde{k}}) >_{L^2(\Gamma)} \\ &= \int_{\Gamma_{\tilde{k}}} a \ \ \overline{\mathcal{F}'(\Gamma_{\tilde{k}})^*\mathcal{R}(\Gamma_{\tilde{k}})}\mathrm{d}s \end{aligned} \tag{4 33}$$

Combining Equation (4 32) and Equation (4 33) yields

$$\int_{\Gamma_{\tilde{k}}} a \ \ \overline{\mathcal{F}'(\Gamma_{\tilde{k}})^*\mathcal{R}(\Gamma_{\tilde{k}})}\mathrm{d}s = -\int_{\Gamma_{\tilde{k}}} a \ \left(\frac{\partial \bar{w}}{\partial n}\frac{\partial u}{\partial n} n\right) \mathrm{d}s, \tag{4 34}$$

which holds for any a Therefore, it follows that

$$\mathcal{F}'(\Gamma_{\tilde{k}})^*\mathcal{R}(\Gamma_{\tilde{k}}) = -\frac{\partial w}{\partial n}\frac{\partial \bar{u}}{\partial n} n \tag{4 35}$$

Using the result of Equation (4 35), the Equation (4 27) can be written as

$$a = -\beta\frac{\partial w}{\partial n}\frac{\partial \bar{u}}{\partial n} n \tag{4 36}$$

Thus, for each iteration, one forward problem from Equation (4 16)-(4 17) and one adjoint problem from Equation (4 28)-(4 29) are solved Once a is determined, $\Gamma_{\tilde{k}}$ is updated by $x + a$ using Equation (4 18)

4 3 Iterative Algorithm

The algorithm of iterative method is as follows

1 Input the *real shape* and *initial guess*

2 Set *numerical shape* to be *initial guess*

3 Solve forward problem at wave number k to obtain the

(a) *real shape* response matrix P_k

(b) *numerical shape* response matrix Q_k

4 Find the residual between P_k and Q_k

5 Use the residual to solve the adjoint problem

6 Obtain the velocity vector

7 Use the velocity vector to update the *numerical shape*

8 Repeat Steps 2-7 until residual is sufficiently small

9 Depending on the detail level of the object, increase k to a corresponding level

Figure 4 1 shows the flow diagram of the iterative method

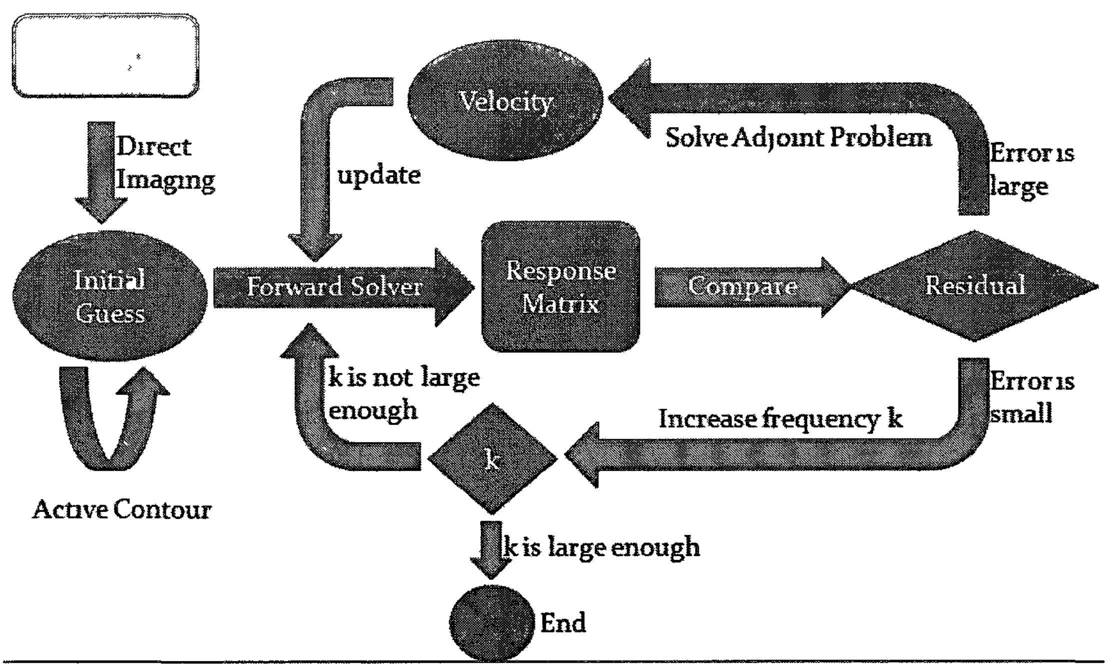

Figure 4 1 Flow diagram of the iterative method

4 4 Numerical Experiments

In the numerical experiments, the solid line is the real shape and the line with crosses is the numerical shape Each cross is a sample point on the boundary and the numerical boundary is obtained by trigonometric interpolation

For the first example, the real shape is a flower with three leaves Figure 4 2 is the initial state, the residual is 0 0088 at $k = 1$ Figure 4 3 is the middle state after 64 iterations, the residual is 0 0031 at $k = 1$ Figure 4 4 is the final state after 128 iterations, the residual is 0 0005 at $k = 1$

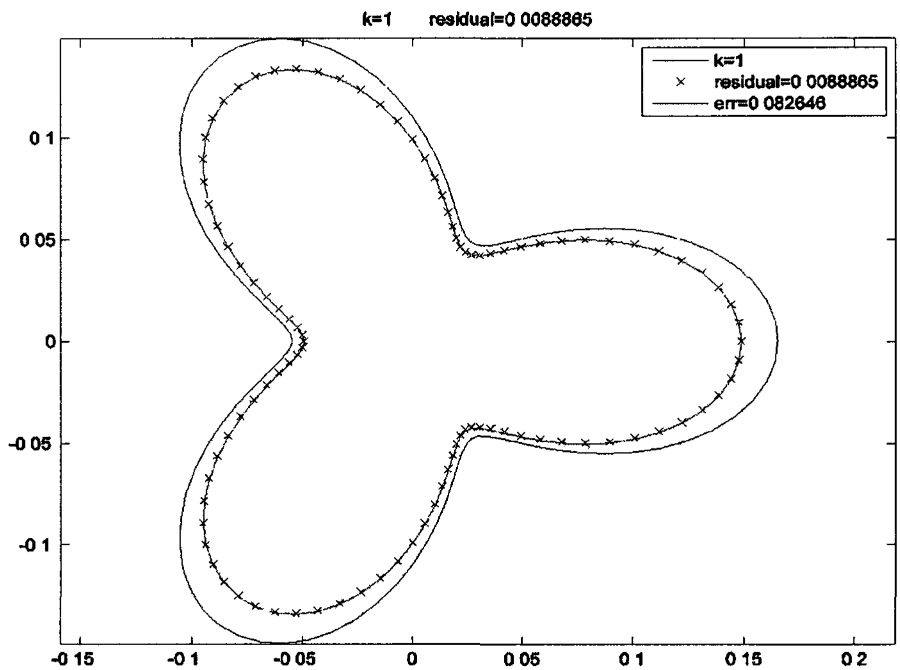

Figure 4 2 Iterative method experiment Flower, initial

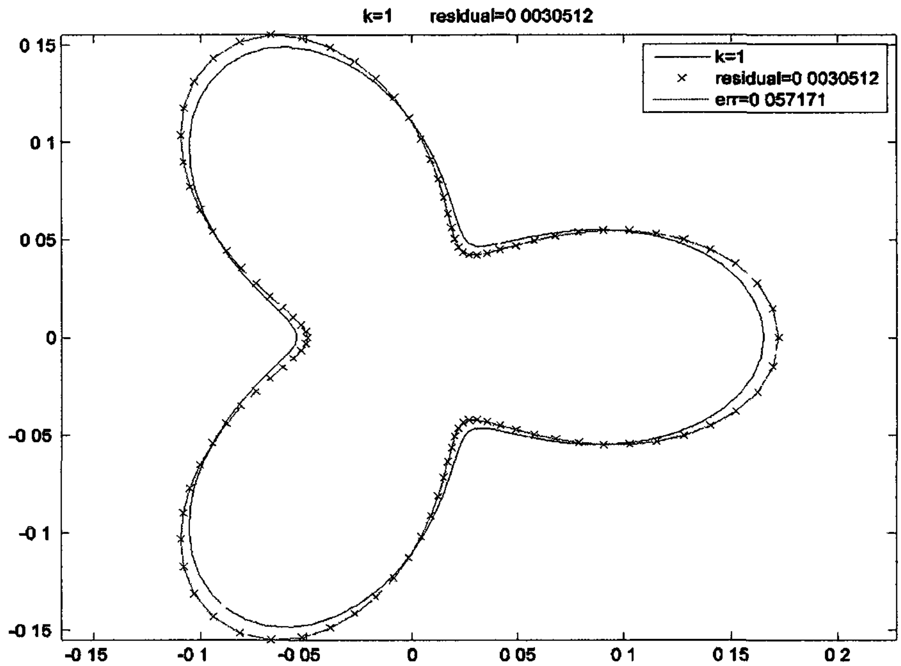

Figure 4 3 Iterative method experiment Flower, middle

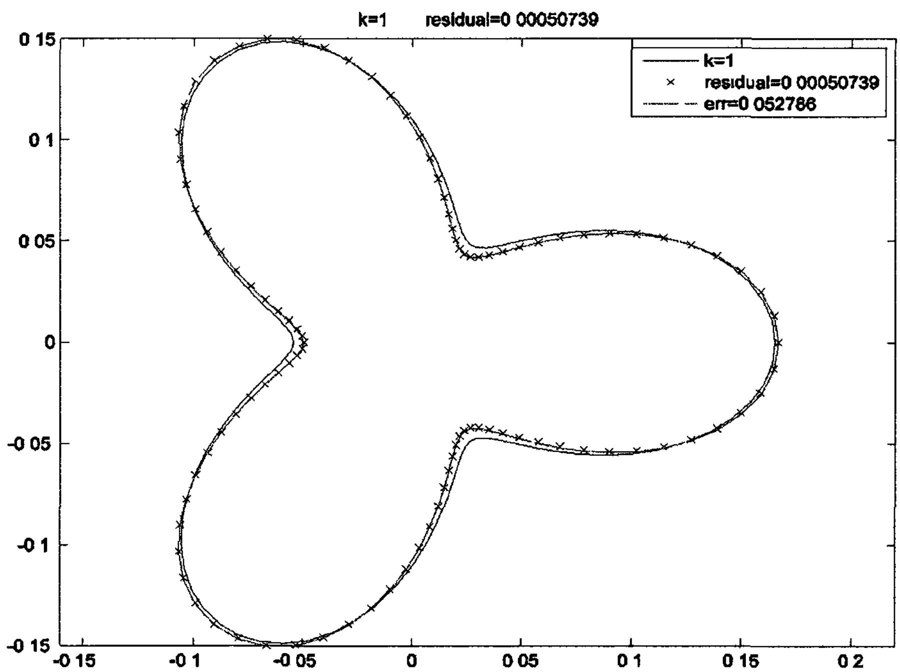

Figure 4 4 Iterative method experiment Flower, final

In the second example, two flowers are placed in the same domain to test the iterative algorithm on multiple targets

Figure 4 5 is the initial state, the residual is 0 0147 at $k = 1$ Figure 4 6 is the state at Step 30, the residual is 0 0147 at $k = 1$ Figure 4 7 is the state at Step 60, the residual is 0 0143 at $k = 1$ Figure 4 8 is the state at Step 75, the residual is 0 0324 at $k = 2$ Figure 4 9 is the state at Step 78, the residual is 0 0216 at $k = 2$ Figure 4 10 is the state at Step 81, the residual is 0 0127 at $k = 2$

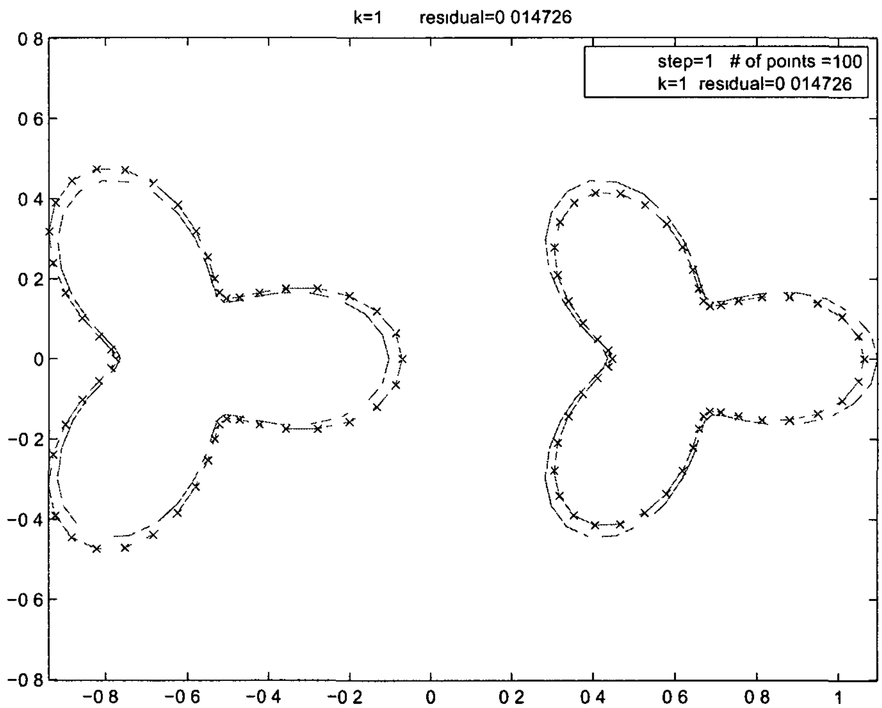

Figure 4 5 Iterative method experiment for two flowers (a)

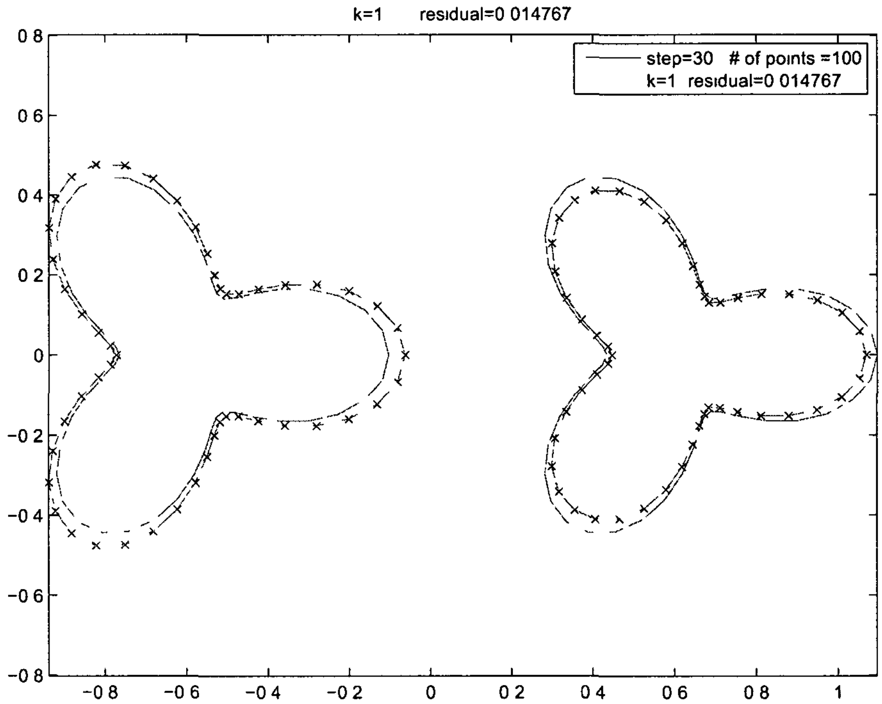

Fıgure 4 6 Iteratıve method experıment for two flowers (b)

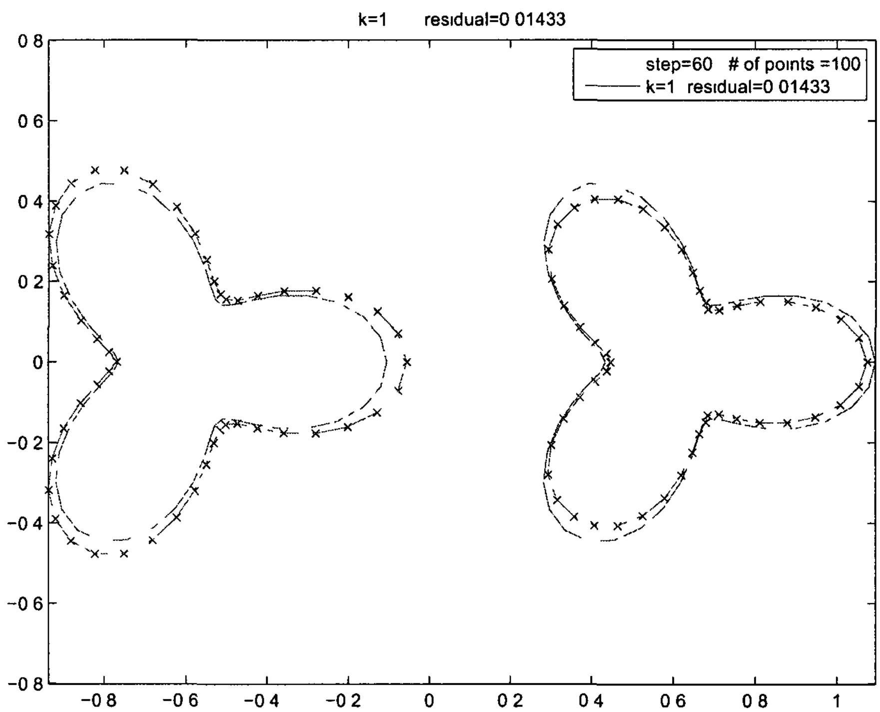

Fıgure 4 7 Iteratıve method experıment for two flowers (c)

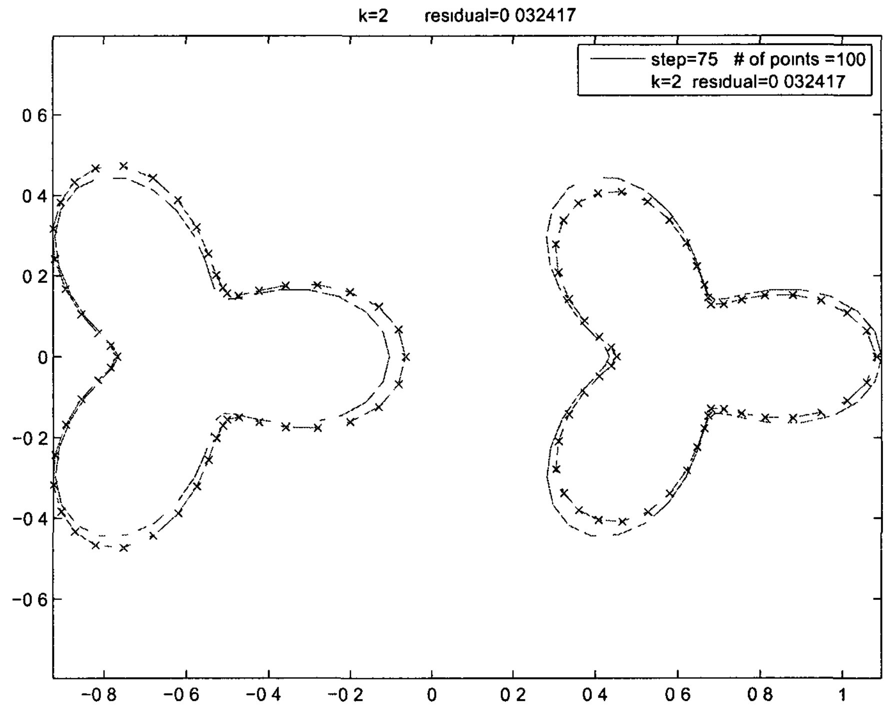

Figure 4 8 Iterative method experiment for two flowers (d)

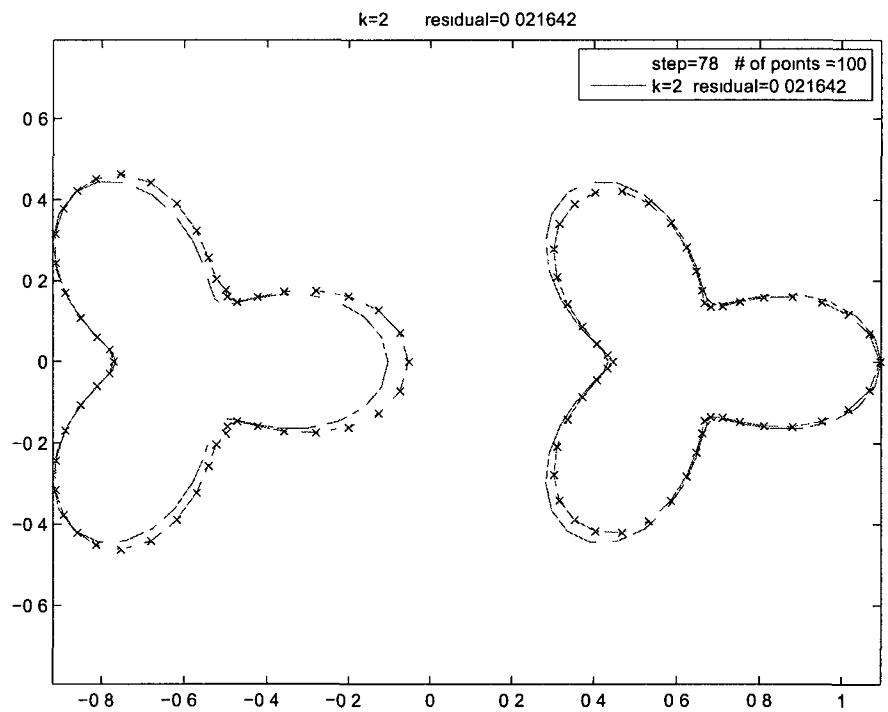

Figure 4 9 Iterative method experiment for two flowers (e)

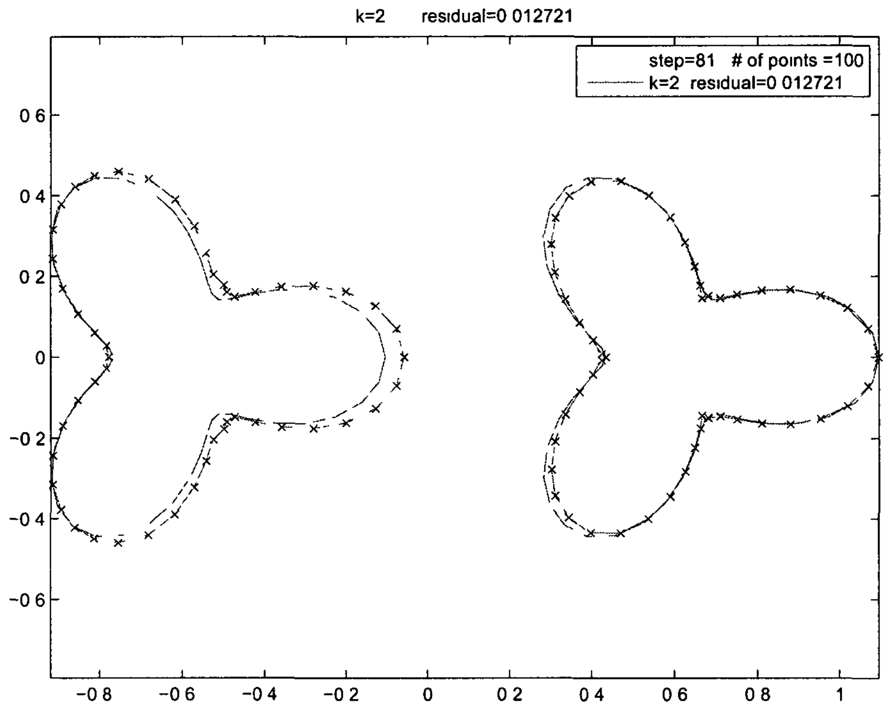

Fıgure 4 10 Iteratıve method experıment for two flowers (f)

It can be seen that ın the second example the resıdual converges slow at wave number $k = 1$ and suffıcıently fast at $k = 2$, whıch means that $k = 1$ can not capture the detaıls of the boundary Wave frequency needs to be ıncreased to guarantee convergence

4 5 Summary for Iterative Imaging

The iterative method is based on MUSIC algorithm for the initial guess to guarantee convergence Image processing is used for converting the MUSIC imaging function into a level set representation for the initial guess and feeding it to the forward solver The recursive linearization solves one forward and one adjoint problems in each iteration step and it is always started from the low-frequency number k and increased k in iteration to capture more details of the boundary of the object The final result is more accurate than just using the direct imaging method The iterative method needs more computation but the forward solver can be parallelized to increase speed

CHAPTER 5

SHAPE CLASSIFICATION

Shape identification and classification has wide applications The crucial thing is to characterize a shape using finitely many numbers In this chapter, we will discuss the relation between response matrix and the geometry of the target A novel method will be proposed that uses the scattering relation and the response matrix We will define a distance function based on the response matrix to compare shapes, study the property of the response matrix under different wave frequency, and apply our distance function on large data set to obtain the retrieval rate

5 1 Basic Concepts

By sending a plane wave from different angles and recording the far field data in different angles, the response matrix is formed The Nystrom method can be used to generate the response matrix by solving the Helmholtz equation In [14], an algorithm for shape classification is proposed using the Poisson equation The method is capable of classifying shapes with some rare mistakes However, unlike the Helmholtz equation, the Poisson equation does not have scaling information

In this chapter, two kinds of objects are used the opaque object and the transparent object For an opaque object, only the boundary of the object is considered The Dirichlet boundary condition is used on the boundary of the object For a transparent object, the whole region of the object is considered The born-approximation method is used to generate the response matrix

The outline of this chapter is as follows Section 5 2 explains how the response matrix is generated and describes the properties of the singular value decomposition of the response matrix Section 5 3, proposes different algorithms for shape classification Numerical experiments are presented in Section 5 4-5 8

5 2 Response Matrix and Singular Value Decomposition

As input, some type of characterization of a shape is needed One way is to give the coordinates of a set of sample points on the boundary of a shape Another way is to give a picture (e g , a "* bmp" file), and image processing can also be used to generate the coordinates of a set of sample points on the boundary

The active contour method developed by Tony Chan et al [6] solves an optimization problem and evolves a curve using the level set method to generate a level set function that has the boundary of the shape as the zero level set Based on this function, a MATLAB command, "coutourc", can be used to generate a set of sample points on the boundary of the shape The trigonometric interpolation, which is introduced in Chapter 4, will be also used here to generate the first and second derivatives

A source at the i-th transducer generates a scattered field that is recorded at the j-th transducer to form one element of the response matrix Changing i, j generates the response matrix The forward solver in Chapter 2 can be used here to generate the response matrix for any shapes

In the numerical experiments, far field data is used instead of near field, that is, to send plane wave from the i-th direction and record far field pattern at the j-th direction to obtain an element of the response matrix The advantage of using far field data is that the location of the array of transducers does not need to be considered and it is easier to compute the far field data

Another method to get the response matrix is born approximation This method can be used on transparent objects, i e , photo images First, the image which contains the object should be represented as a matrix Each pixel in the image is mapped to a corresponding value in the matrix to represent the brightness of that pixel Then, the integration of the product of two Green's functions generates one element of the response matrix

For the near field pattern, the response matrix P is obtained by

$$P_{ij} = \int_D \sigma(y) G(x_i, y) G(x_j, y) dy, \tag{5 1}$$

where x_i is the location of the source of coming wave, and x_j is the location of the receiver of the scattering wave $G(x, y)$ is Green's function In two-dimensional case

$$G(x, y) = \frac{i}{4} H_0^1(k\|x - y\|), \tag{5 2}$$

and in three-dimensional model

$$G(x, y) = \frac{e^{ik\|x-y\|}}{4\pi\|x - y\|}, \tag{5 3}$$

The $\sigma(y)$ is an arbitrary function $\sigma \quad D \to \mathbb{R}$, e g $\sigma \quad D \to [0, 255]$ can be defined to indicate the contrast of a image

For far field pattern, the response matrix P is obtained by

$$P_{ij} = \int_D \sigma(y) e^{iky\, d_i} e^{iky\, d_j} dy, \tag{5 4}$$

where d_i is the direction (unit vector) of incident wave, and d_j is the direction of scattering wave

Born approximation is faster than the Nystrom method since the Hankel function does not need to be computed in the formula of born approximation

The shape information is embedded in the response matrix The dominant information is embedded in the first few singular vectors of the response matrix To reduce storage from $O(n^2)$ to $O(n)$, only the first few singular values or vectors are stored Now each shape is encoded by $O(n)$ numbers, where n is the number of angles

5 3 Algorithms for Shape Classification

The basic algorithm for shape classification using response matrix information is as follows

1 Input image file

2 Take the imaging processing to obtain a level set function

3 Generate sample points on the boundary

4 Interpolate using trigonometric functions to generate locations and first and second order derivatives

5 Compute the perimeter and rescale it

6 Find the center of mass of the shape and relocate

7 Find the minimal sample points on the boundary that guarantee the accuracy of the forward problem

8 Compute the response matrix (might add noise)

9 Use SVD for shape classification

To take care of a shift, the centroid of the shape is computed using the sample points on the boundary This can be done by viewing the shape as a combination of signed triangles formed by neighboring sample points and a fixed reference point since the centroid of a triangle can be easily computed

To take care of a scaling, the perimeter of the shape is computed and normalized For the Born Approximation problem, the area of the shape is computed and normalized

To take care of a rotation, essentially a shift of the index is done for the response matrix The simplest idea is to search among all possible shifts and compute a norm of the difference between the matrix of the reference shape and the matrix after the index shift of the shape to be tested However, this method has two disadvantages first, it is not robust, second, it needs a storage of $O(n^2)$ If only the singular value is used to compare, the shifting is not needed since the singular value of a matrix is identical while shifting the row and column

To take care of contrast variance, the $\sigma(x)$ is normalized using Frobenius-norm

5 4 Response Matrix by Forward Solver using Nystrom Method

First, examples where the shapes are generated from a picture are considered, for example, a bmp file for a solid simply connected region The procedure described in Section 5 2 is used to generate sample points on the boundary and the first and second derivatives The Nystrom method is used to obtain the response matrices for these shapes

The reference shape is set as a Chinese character "Wang" with bold font Shape 1 to be tested is the same shape with scaling and rotation Shape 2 is the same Chinese character "Wang" with another font (Songti) Shape 3 is a Chinese character "Zheng" with bold font The results in Figures 5 1 - 5 4 show that Shape 1 is the only correct shape

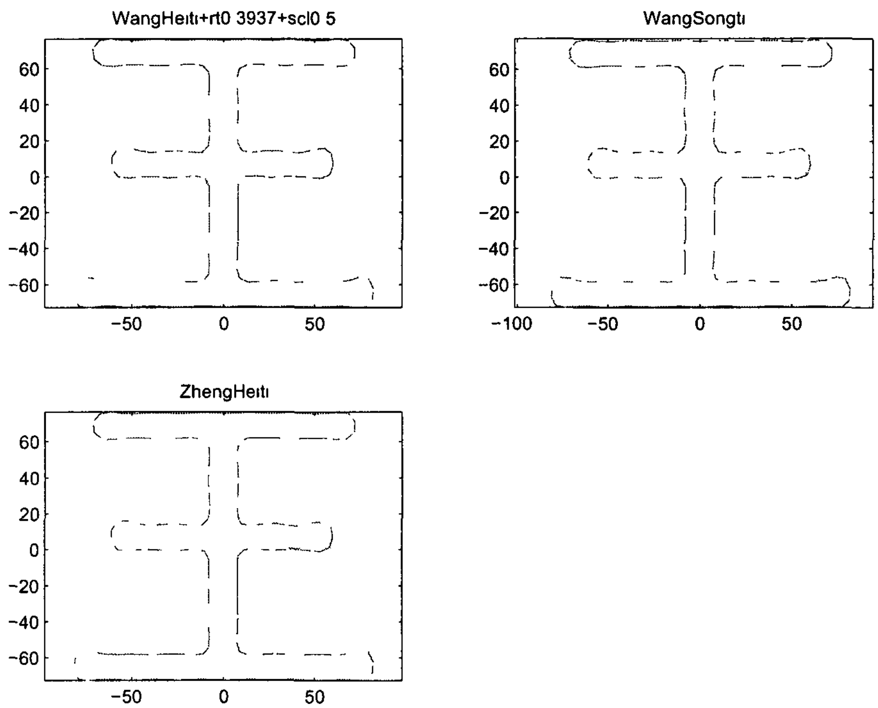

Figure 5 1 Chinese character comparison

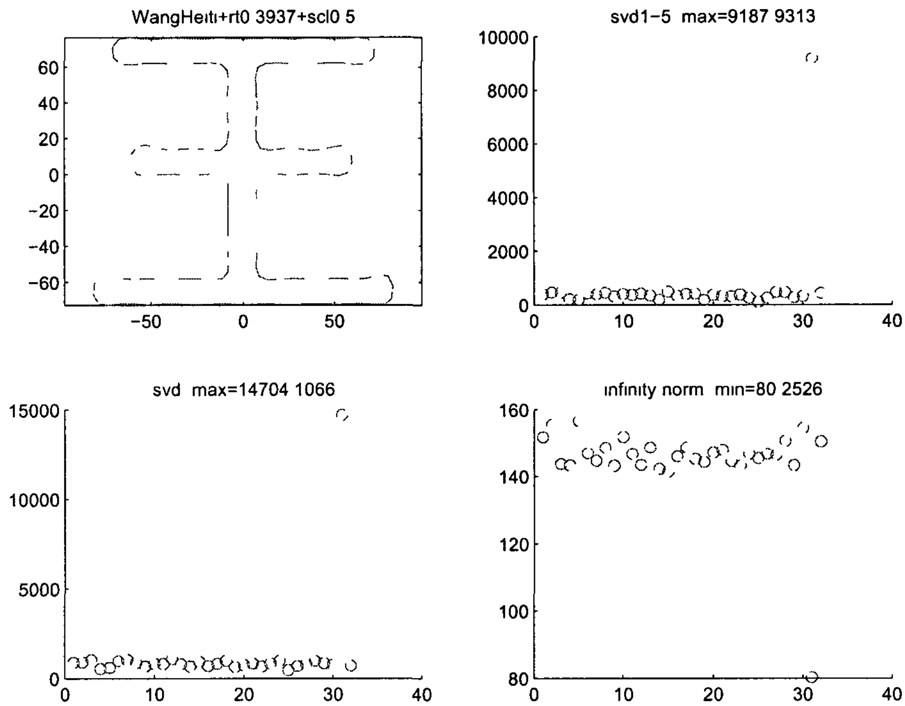

Figure 5 2 Chinese character comparison, matched case

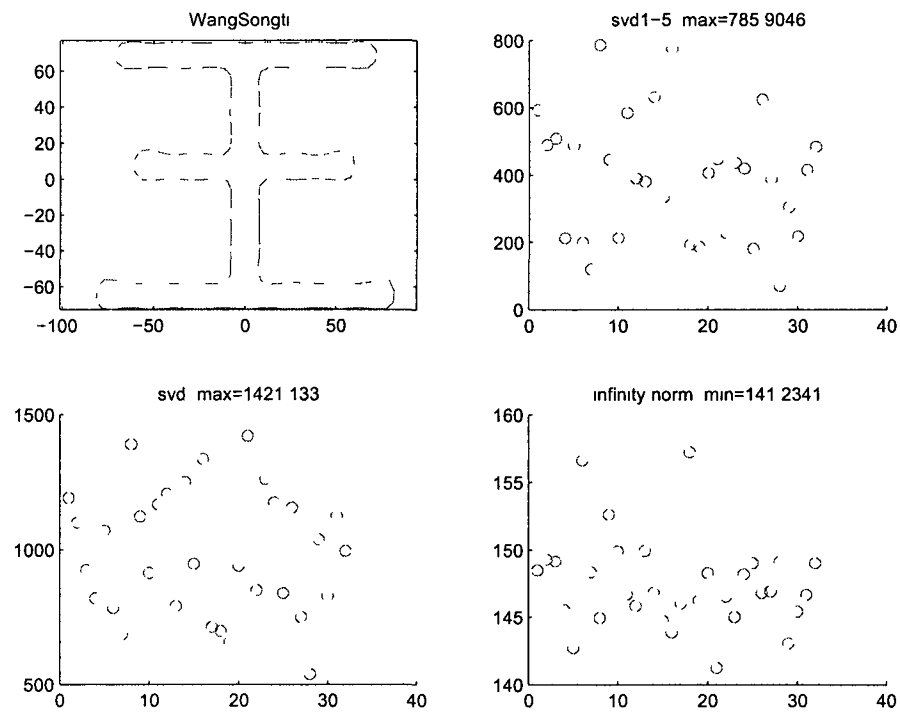

Figure 5 3 Chinese character comparison, different fonts

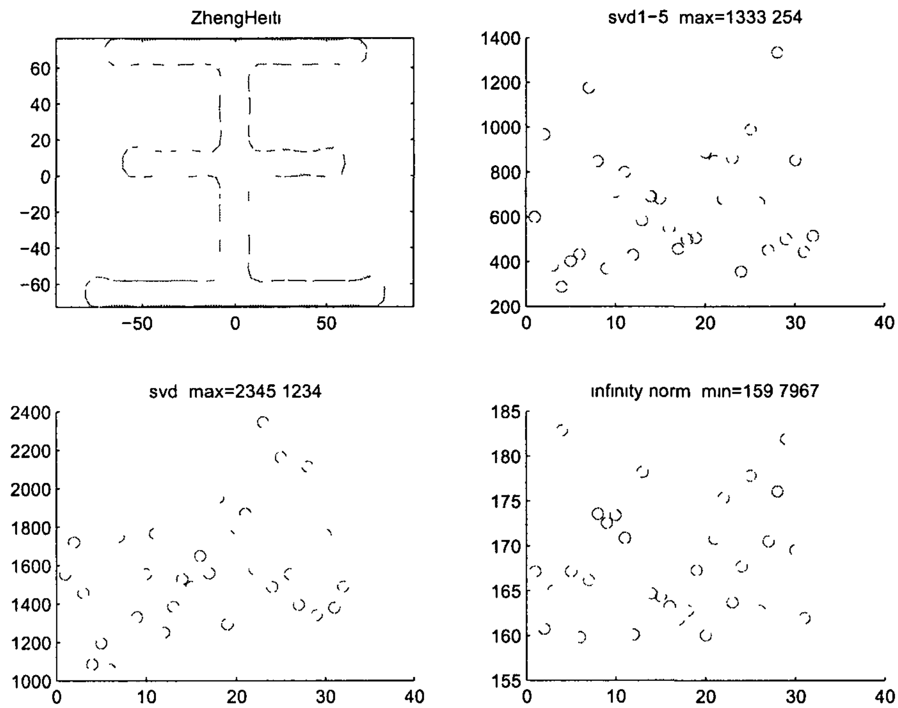

Figure 5 4 Chinese character comparison, different characters

Next, the reference shape is set to be a spiral curve, see Figure 5 5 Shape 1 is the same shape with a rotation of 0 3937(radian measure) and a scaling of 0 5 Shape 2 is a shorter spiral that matches with the reference shape except at the tip Again, the result in Figure 5 6 and Figure 5 7 show that the correct shape could be identified

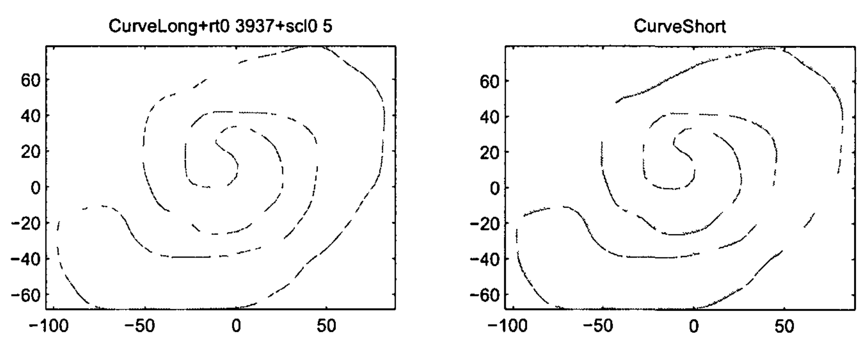

Figure 5 5 Curve comparisons

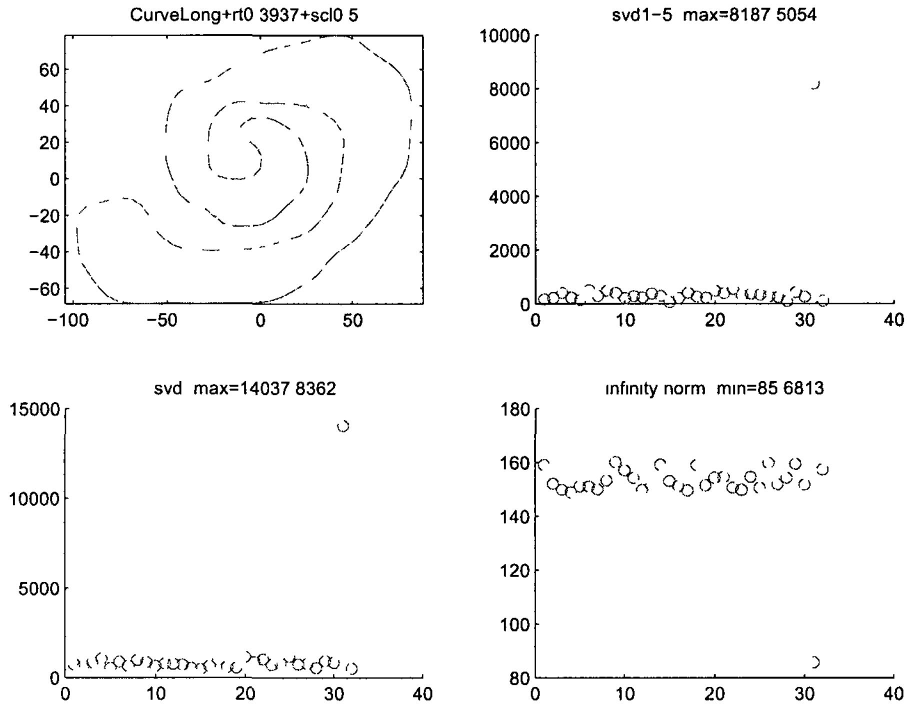

Figure 5 6 Long curve v s long curve

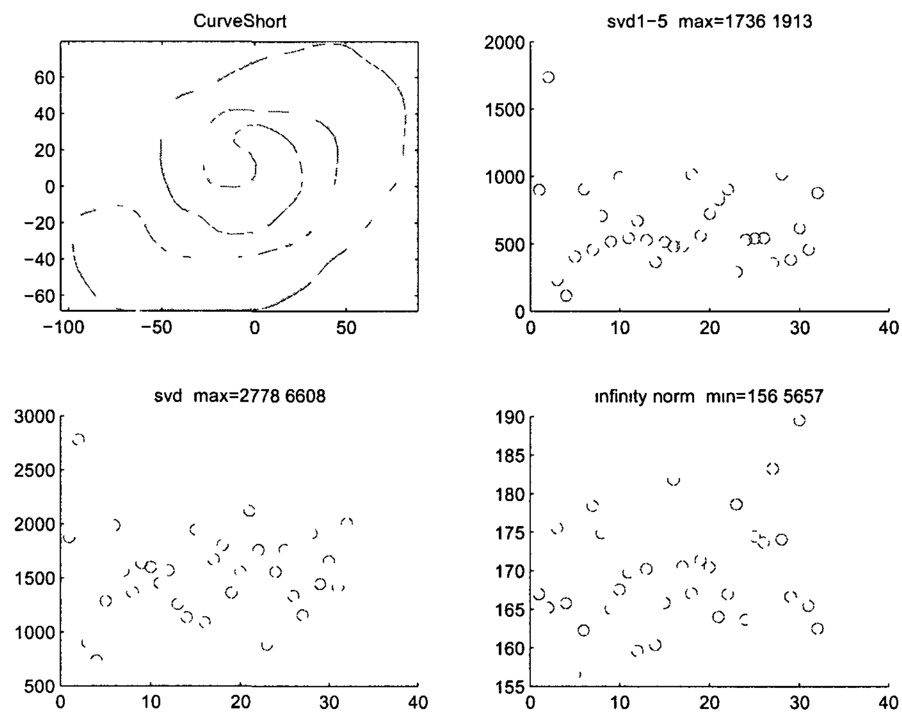

Figure 5 7 Long curve v s short curve

Next, a library was build to contain the shape information of a group of reference shapes For each reference shape, only the first five eigenvalues of the corresponding response matrix was stored Given a reference shape, users can go through the library to find the same shape

Figure 5 8 and Figure 5 9 show a search for the bold font Chinese character "Wang" in the library The sixth comparison in Figure 5 8 is a correct match with a peak value 157, which is much larger than other peak values

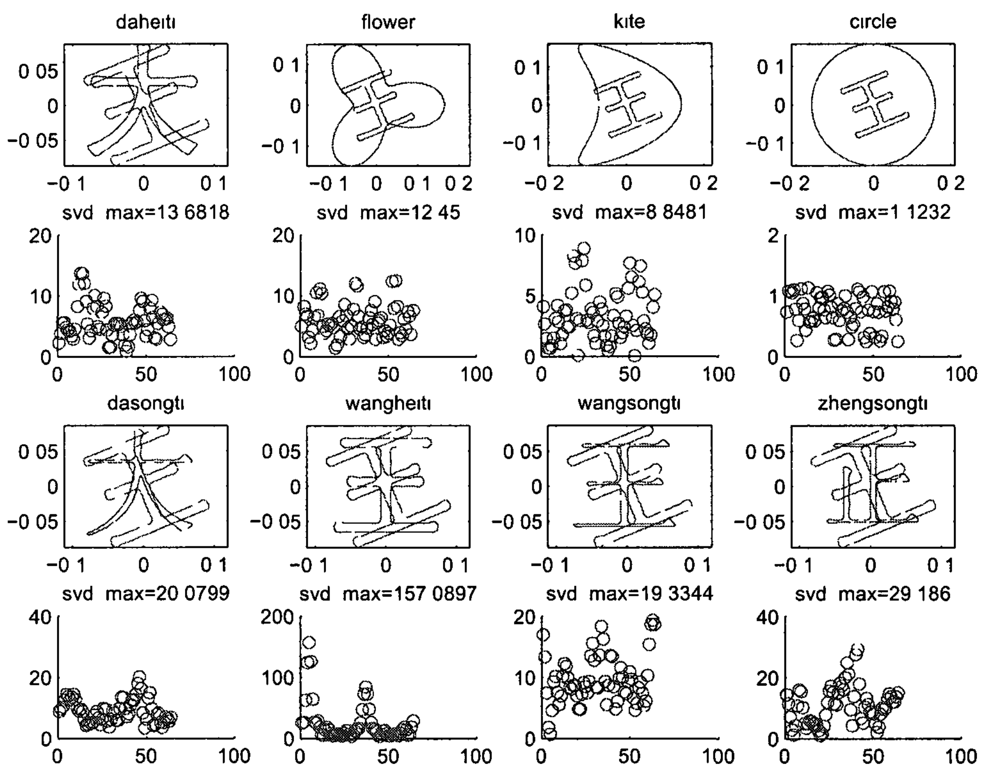

Figure 5 8 Search "Wang" in library, no noise

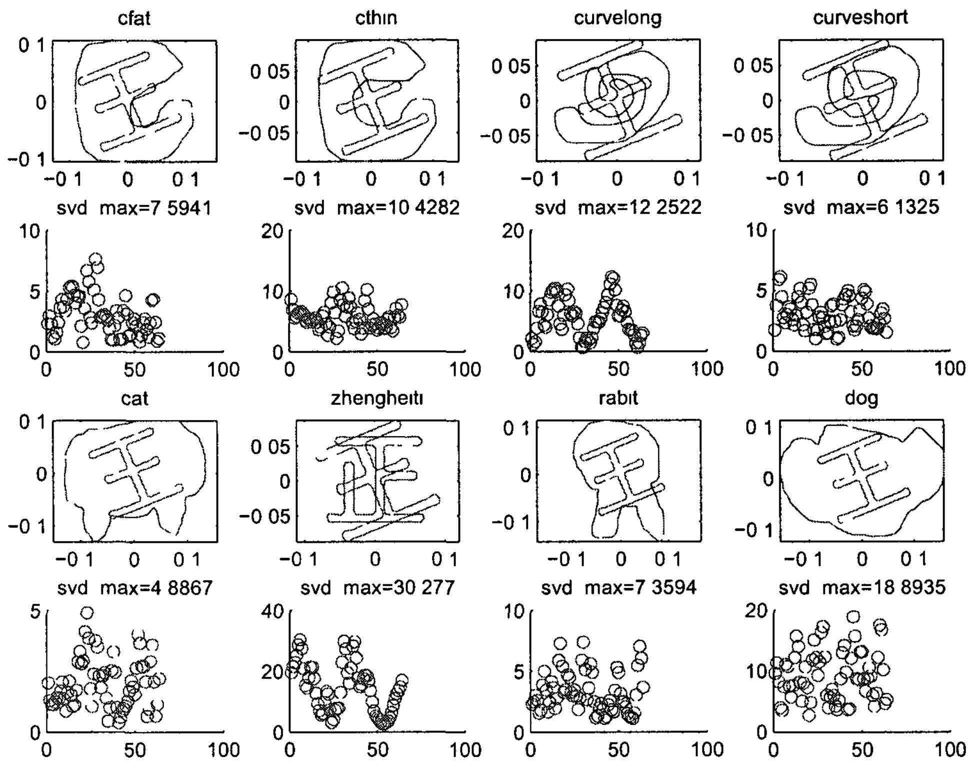

Figure 5 9 Search "Wang" in library, no noise

The advantage of usıng the SVD method to compare ıs robust Fıgure 5 10 and Fıgure 5 11 show the result of addıng 50% noıse The sıxth comparıson ın Fıgure 5 10 ıs a correct match wıth a peak value 90, whıch ıs much larger than other peak values

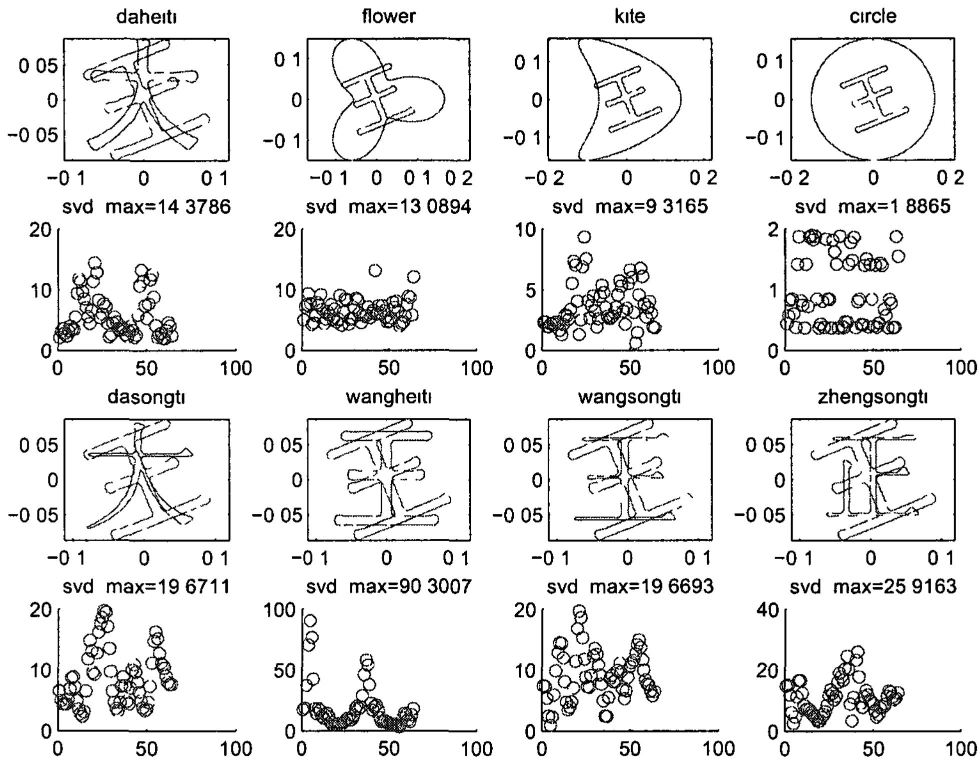

Fıgure 5 10 Search "Wang" ın lıbrary wıth 50% noıse, part 1

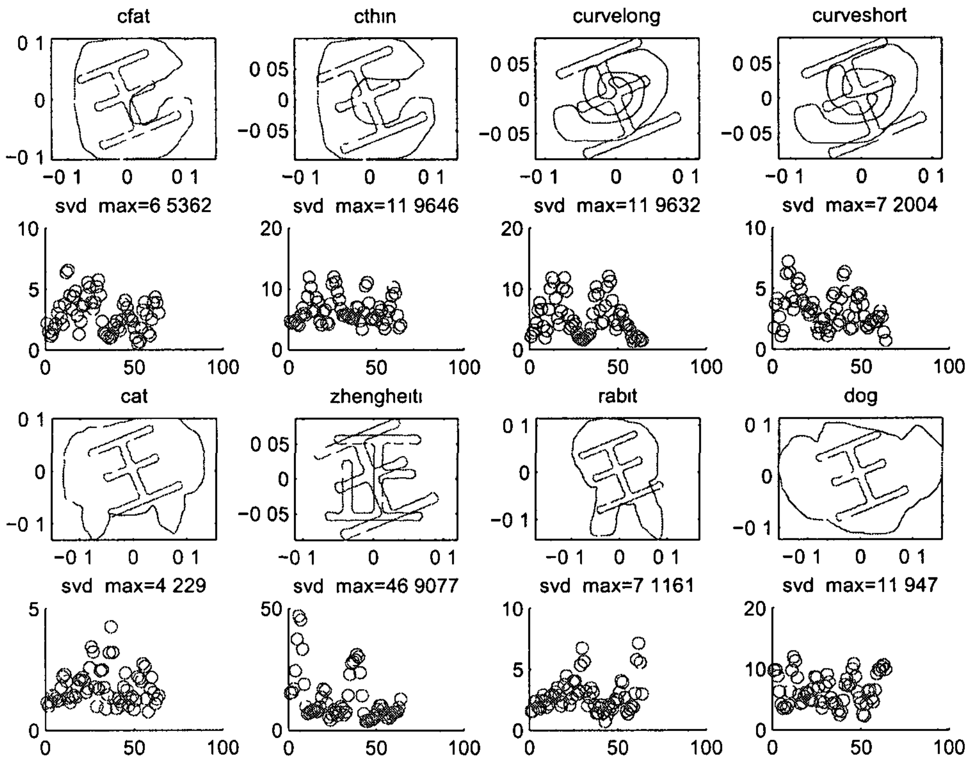

Figure 5 11 Search "Wang" in library with 50% noise, part 2

Then, the noise is set to be biased noise Figure 5 12 and 5 13 show the result The sixth comparison in Figure 5 12 is a correct match with a peak value 237, which is much larger than other peak values

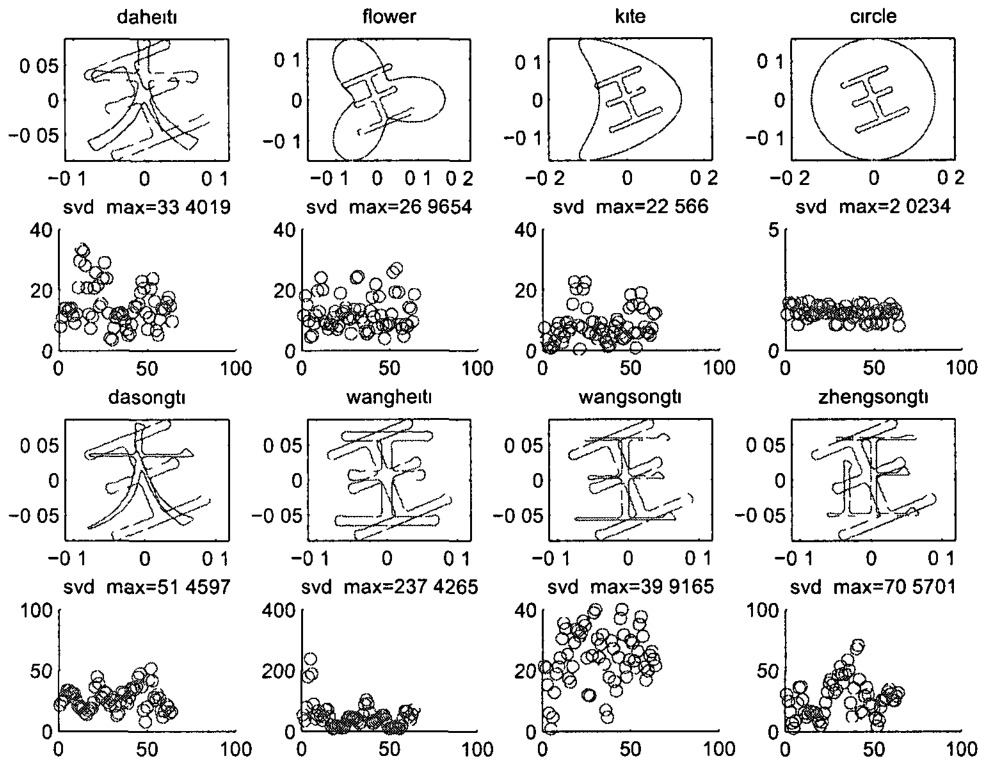

Figure 5 12 Search “Wang” in library with 50% biased noise, part 1

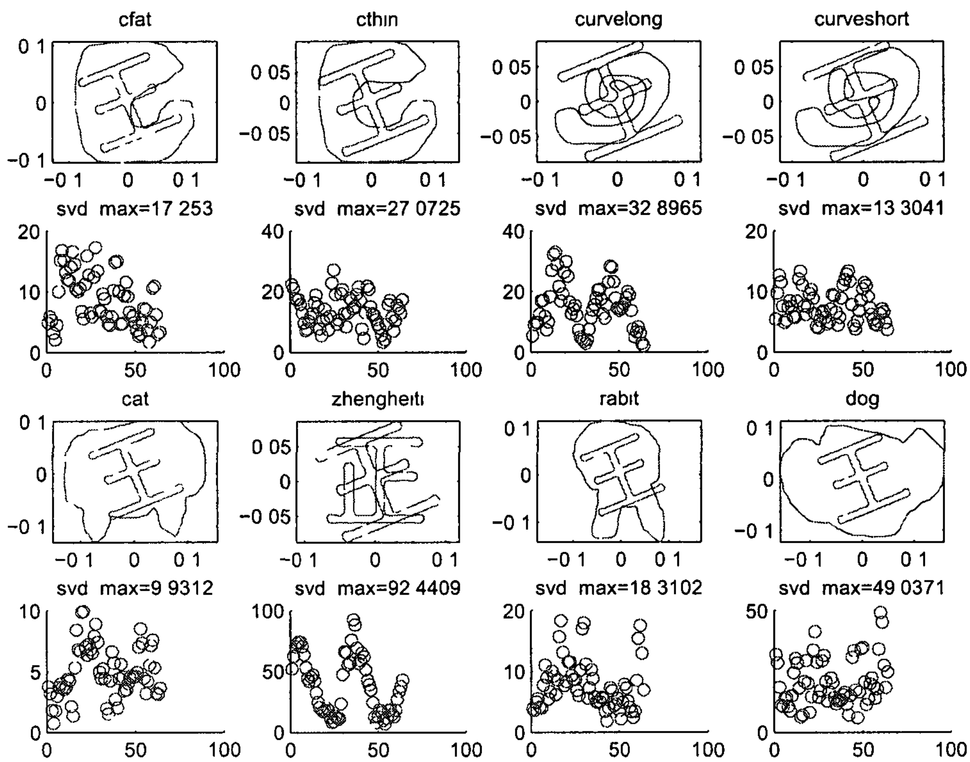

Figure 5 13 Search "Wang" in library with 50% biased noise, part 2

5 5 Response Matrix by Born Approximation

This section shows the results of shape classification using response matrices based on Born approximation

First the response matrices were generated using Born approximation for the data set at wave frequency $k = 20$ For example five different classes of shapes are used "apple", "bat", "bird", 'cup", "Heart", each class contains five shapes "apple-1" was used as a reference shape and compared the distance between every shape and "apple-1"

The distance function is

$$d_1(s_1, s_2) = ||svd(r(s_1)) - svd(r(s_2))||_2, \tag{5 5}$$

where $r(\ )$ is the response matrix generated by born approximation, and $svd(\ )$ gets the singular values of a matrix

The results are shown in Figure 5 14 All the figures are listed in an increasing distance order Five apples are in the top five The other four classes are grouped together

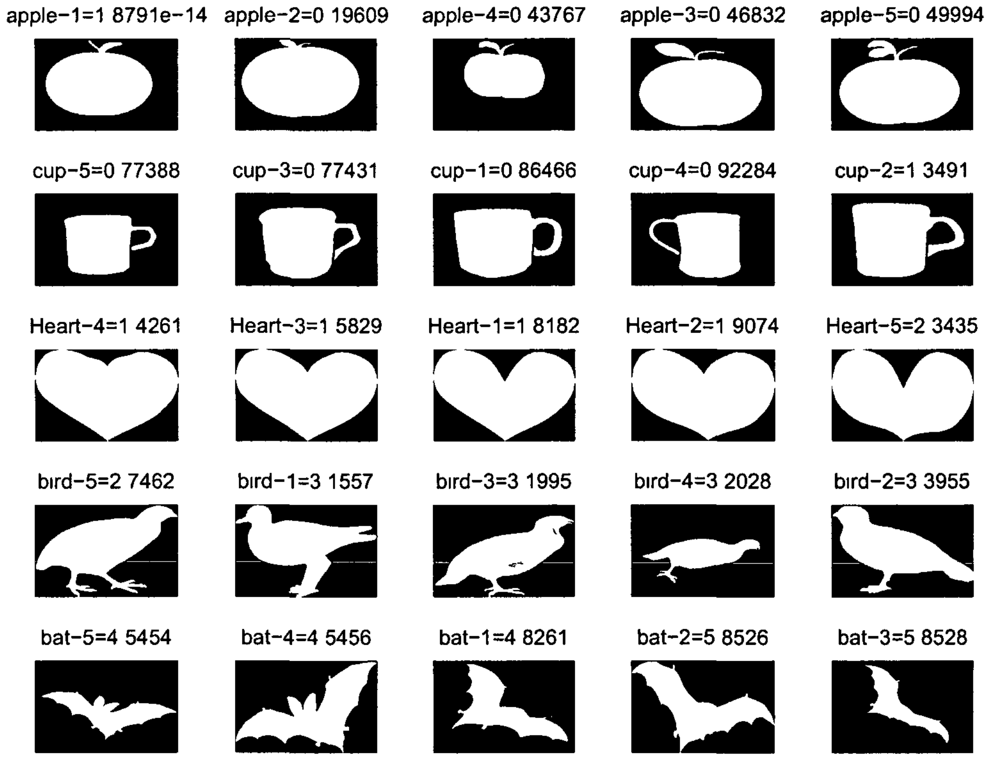

Figure 5 14 Reference shape "apple-1"

If “bat-1” is taken as reference shape, the results are shown in Figure 5 15 Although “cup-2” is mixed with “Heart-4”, the five bats are still in the top five

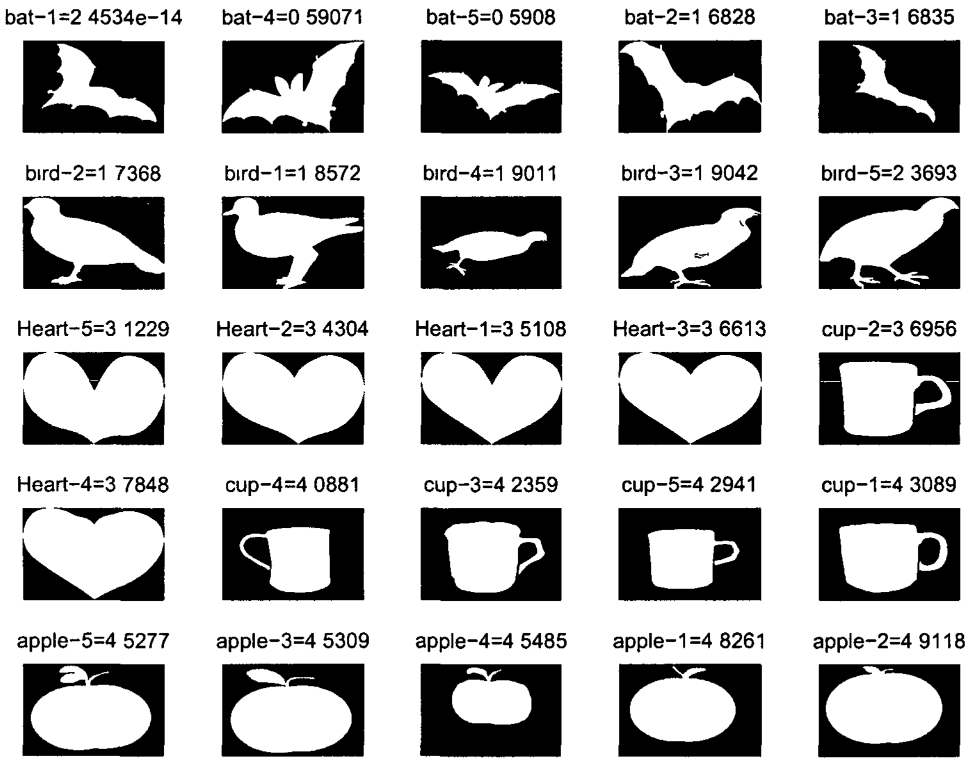

Figure 5 15 Reference shape “bat-1”

Figure 5 16 uses “lizard-1” as a reference shape All five lizards are in the top five Although the “snake” shape is similar to the “lizard” shape, the current method can still distinguish them

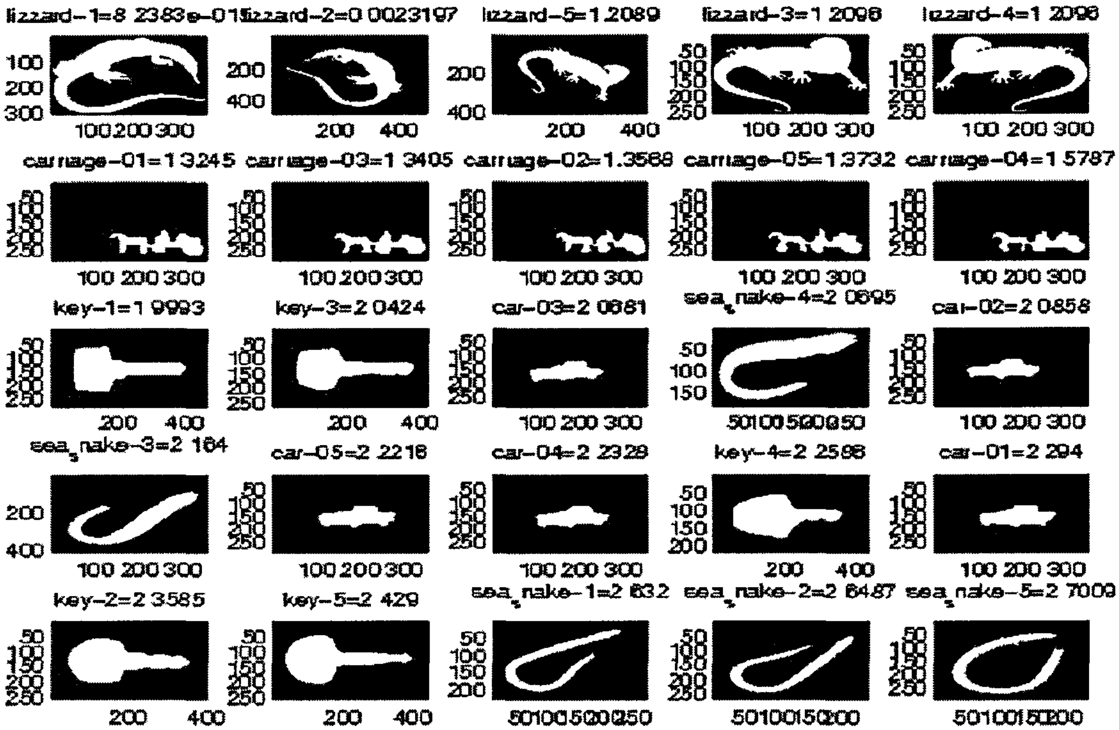

Figure 5 16 Reference shape “lizard-1”

Figure 5 17 shows the result of comparing different Chinese characters in different fonts The same characters to the reference character are in the top five

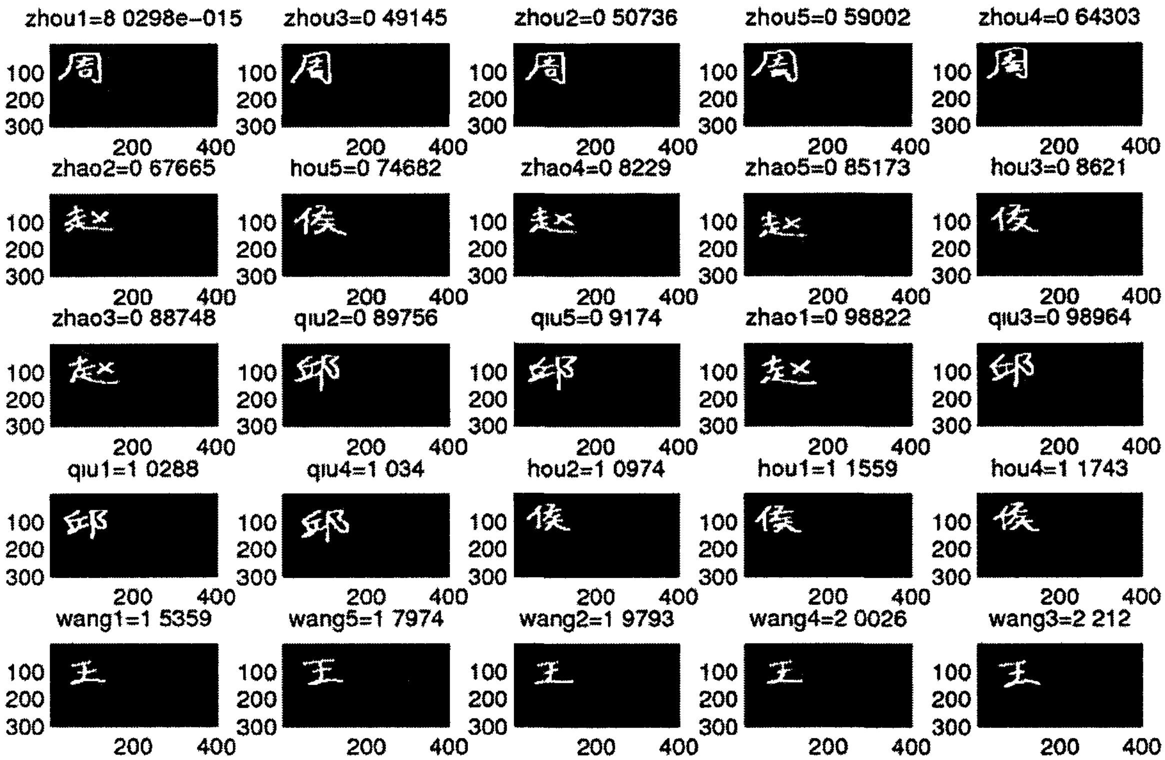

Figure 5 17 Reference shape Chinese characters

5 6 Frequency Fılterıng

The born approxımatıon ıs sımılar to fourıer transformatıon The geometrıc domaın ıs mapped to the frequency domaın Fıgure 5 18 shows the frequency dıstrıbutıon

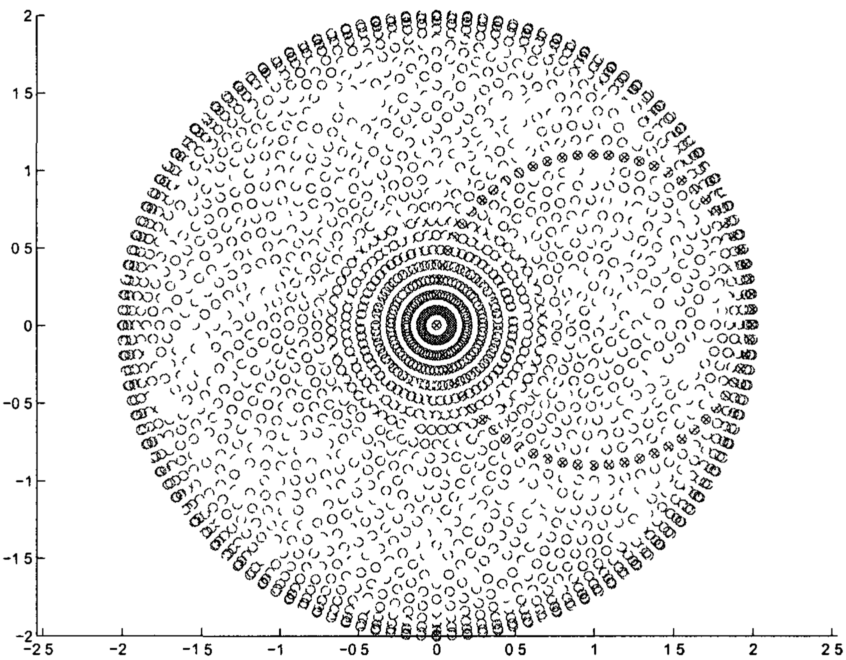

Fıgure 5 18 Frequency dıstrıbutıon

The dots wıth cross ın Fıgure 5 18 form one column of the orıgınal matrıx The low frequency part ıs ın the center and vıce versa The low frequency part or hıgh frequency part can be truncated based on the demands Then, the response matrıx can be reformed by the ıncreased or decreased frequency order to get a better result

A data set of dıfferent kınds of flower shapes ıs consıdered, as shown ın Fıgure 5 19 There are five classes ın the data set, and each class contaıns five shapes Shapes ın thıs data set are classıfied by the number of leaves

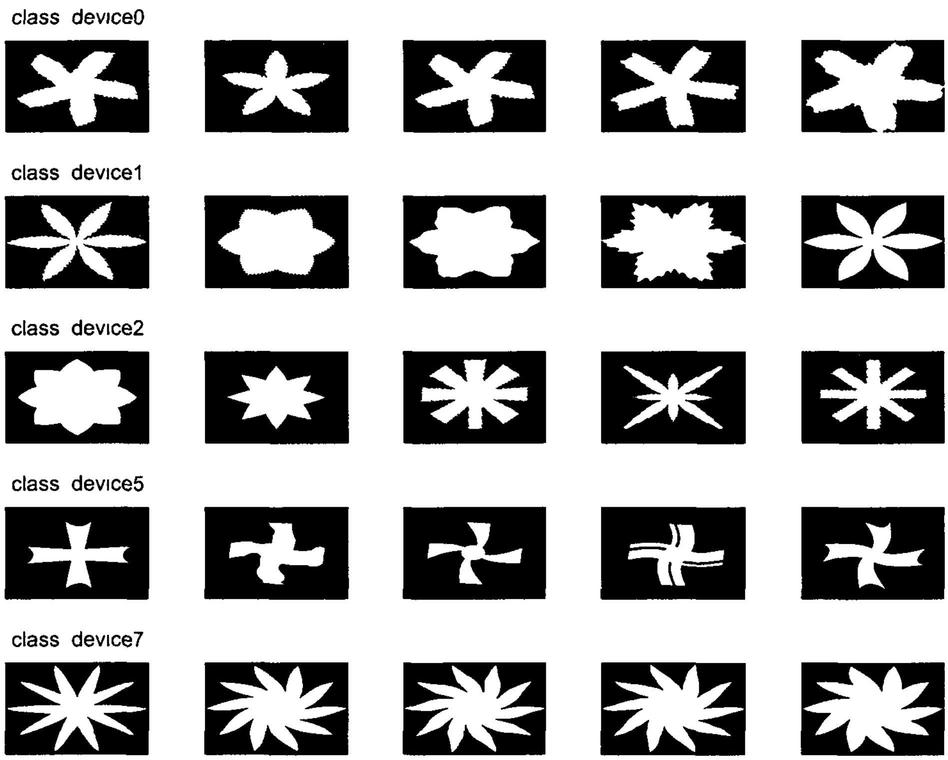

Figure 5 19 Five classes Original

Figure 5 20 shows the results using distance function d_1 The distance function d_1 failed on this data set

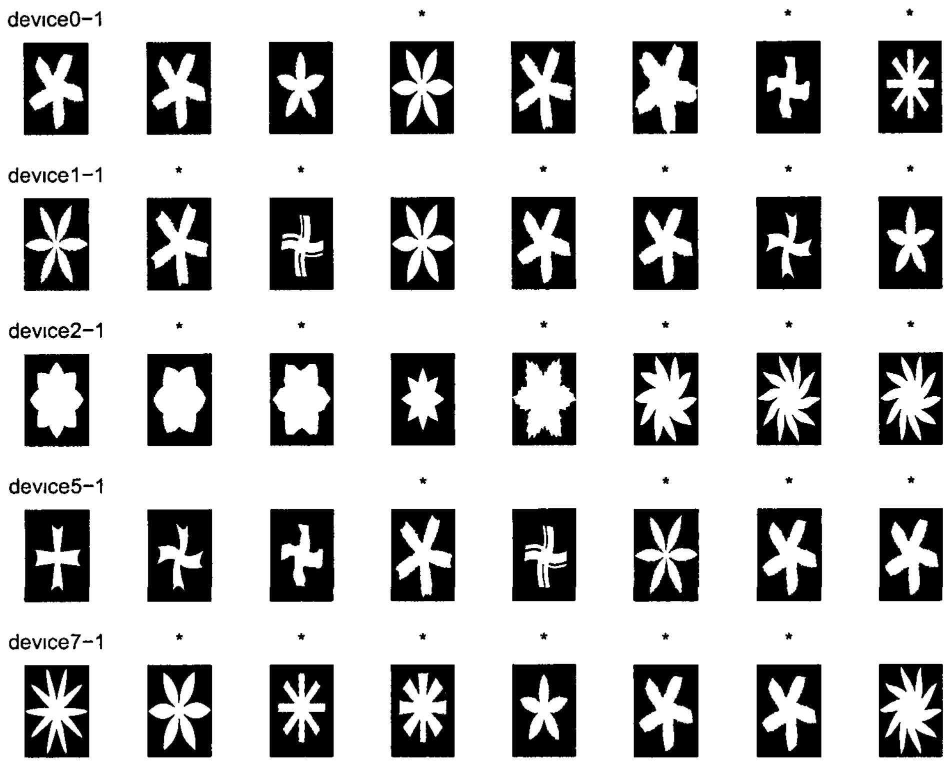

Figure 5 20 Five classes using distance function d_1

In Figure 5 20, "device0-1", "device1-1", "device2-1", "device5-1", "device7-1" is taken as the reference shape separately, compared with other shapes in the set The top eight matches are shown The shape which is in a different class as the reference shape will be marked with a '*' on the top The result is not as good as in the previous examples Therefore, another metric needs to be found to measure the distance between two shapes, which is introduced by distance function d_2

Let s_1, s_2 be two shapes in the data set r_i is the response matrix of s_i, $i = 1, 2$ Take the singular value decomposition $r_i = U\Sigma V^H$, where $\{u_j^{(i)}\}_{j=1}^n$ and $\{v_j^{(i)}\}_{j=1}^n$ are the singular vectors obtained from U and V Then, the distance between s_1 and s_2 is defined as below

$$d_2(s_1, s_2) = \sum_{i=1}^{n} |(u_i^{(1)} u_i^{(2)}) \overline{(v_i^{(1)} v_i^{(2)})}| \qquad (5\ 6)$$

Here $n = 5$ is set to ignore noise Figure 5 21 shows the result using metric d_2, which is much better than using metric d_1

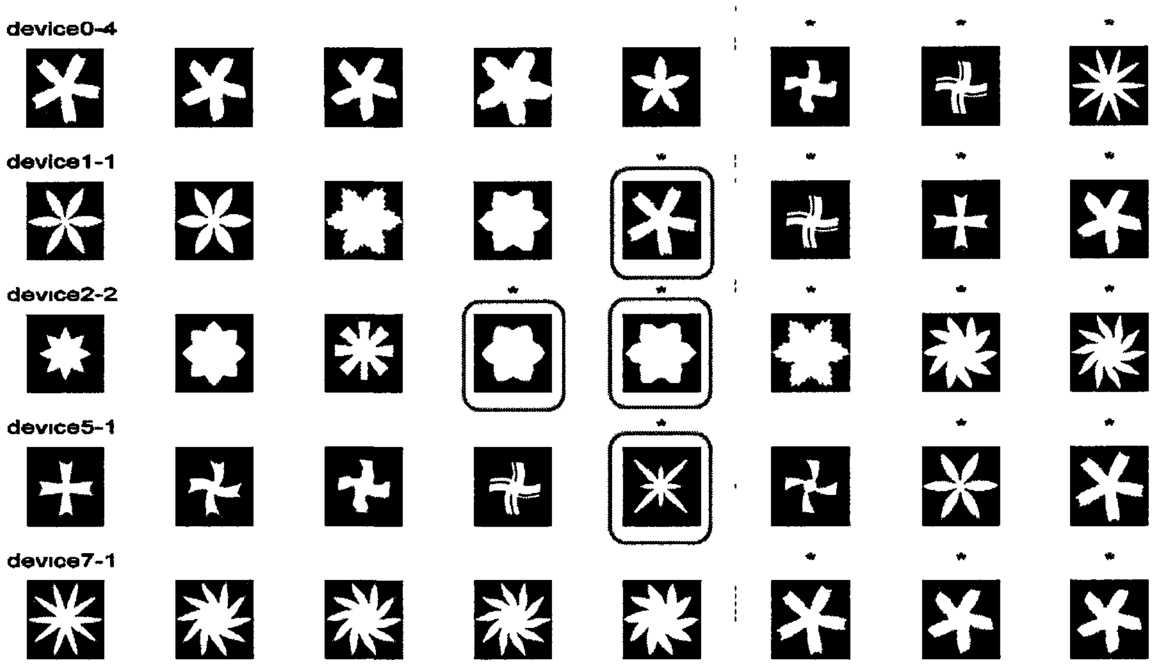

Figure 5 21 Five classes using distance function d_2

5 7 Face Recognition

This section introduces contrast information to a two-dimensional object to represent a gray image, and classification method is applied to identify faces Figure 5 22 shows the result of face recognition using the current distance function based on the response matrix generated by Born approximation The picture of one person is used as a reference shape and compared to all the other pictures The results are placed in a decreasing order The five pictures of the same person are in the top five

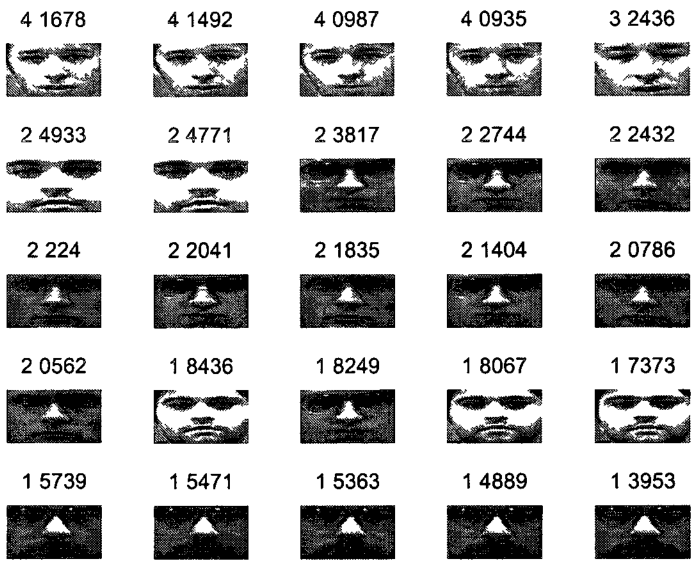

Figure 5 22 Face recognition

5 8 Retrieval Rate on the MPEG-7 Shape Data Set

The MPEG-7 Shape is a standard testing data set of non-rigid shapes with a single closed contour It consists of 70 different classes of shapes and each class contains 20 different shapes The introduction of MPEG-7 Shape data set can be found in [28] The MPEG-7 Shape data set is tested on many classification algorithms to obtain the shape retrieval rate Most of those shape classification method are based on the property of the shapes However, the classification method presented in this chapter is based on the response matrix generated by the shape using the Helmholtz equation Therefore, before computing the shape retrieval rate, the Born approximation is applied on all the shapes in order to obtain the response matrix

In the numerical experiment, we set the wave number k to be $k = 20$ and the number of transducers N to be $N = 64$ Hence, the response matrix P is of 64×64 dimension

The retrieval rate is computed by the so called Bull's eye score

1 Every shape in the database is compared to all other shapes There are totally 1960000 comparisons

2 The number of shapes from the same class among the 40 most similar shapes is reported For this experiment, the reported number is 18569

3 Ratio of the total number of shapes from the same class to the highest possible number is computed as the retrieval rate For this experiment, the highest possible number is $1400 \times 20 = 28000$ Hence

$$\text{ratio} = 18569/28000 \approx 66\ 32\%$$

Figure 5 23 is the example of the 40 most similar shapes for the "apple-1"

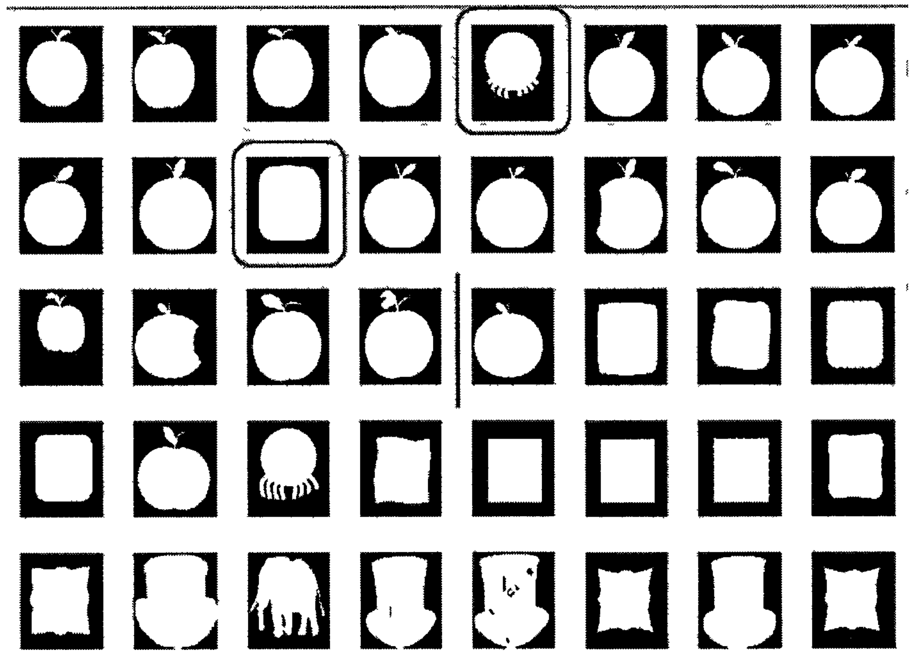

Fıgure 5 23 MPEG-7 comparıson for “apple-1”

The Skeleton DAG method [31] has the retrıeval rate of 60% The Wavelet method [8] has the retrıeval rate of 67 76% The Curvature scale space method [32] has the retrıeval rate of 75 44% The Shape contexts method [3] has the retrıeval rate of 76 51% The Curve edıt dıstance method [41] has the retrıeval rate of 78 17%

Most of the algorıthms are based on the shape ınformatıon Our method, ınstead, ıs based on the response matrıx ınformatıon There are several advantages usıng response matrıx to classıfy shapes

1 No specıal treatment needed for shape scalıng and rotatıon

2 The storage ıs effıcıent sınce the forward solver or the Born approxımatıon maps the shape from the shape space, whıch ıs a ınfınıte dımensıon space, ınto a complex matrıx space, whıch ıs a fınıte dımensıon space

3 When the shapes cannot be visualized, the physical measurements lead to the scattered field information of the shape Our response matrix generated by solving the Helmholtz equation is accurate comparing to the response matrix obtained from physical measurement Therefore, the scattered field data can be directly fed to our algorithm to compute for the retrieval rate The shape-based algorithms need the shape information which can be only obtained by solving the inverse problem Our method is much faster in this case

5 9 Summary for Shape Classification

Using the response matrix or its singular values and vectors to represent shape is storage efficient This study shows that only the first few singular values and vectors need to be stored and used to characterize the shape The storage is reduced from $O(n^2)$ to $O(n)$ Therefore, a shape can be characterized and a shape library can be built using the least amount of data Shape rotation and scaling can be easily dealt with in the response matrix The wave frequency can be filtered to focus on different detail levels in classification Moreover, the SVD method used is robust to noise The retrieval rate is obtained on MPEG-7 Shape data set

CHAPTER 6

CONCLUSIONS

This dissertation proposed an effective iterative method for inverse problem based on the forward solver for iteration and direct imaging result for the initial guess The Nystrom method is used in the forward solver and adjoint problem The response matrix generated by the Nystrom method converges exponentially with respect to the number of sample points on the boundary of the target Image processing was used for converting the MUSIC imaging function into a level set representation for the initial guess, and was then fed to the forward solver The recursive linearization solves one forward problem and one adjoint problem in each iteration step The process always starts from low-frequency number k and increase k in iteration to capture more details of the boundary of the object Numerical examples show that this method can be applied on single or multiple targets, and the residual of the final state is less than the residual of the initial guess, which means that the result of this iterative algorithm is more accurate than the result of the direct imaging method

The inverse problem was applied to shape identification and classification since there is a relation between the shape itself and the response matrix obtained from the shape The distance function was designed based on the response matrix or its SVD information Index shifting of the response matrix was used to represent the shape rotation Numerical examples shows that the SVD method used is robust to noise Filtering is used to control the detail level of the shapes and is tested on the classification example The classification algorithm is fast, using Born Approximation, and storage efficient, using the distance function on SVD of the response matrix The classification method based on the response matrix is tested on a large data-set (MPEG 7 Shape) and the retrieval rate is computed The method will be also combined with machine learning techniques to improve the retrieval rate in the future

BIBLIOGRAPHY

[1] X Bai, X Yang, L J Latecki, W Liu, and Z Tu Learning context-sensitive shape similarity by graph transduction *IEEE Trans on Pattern Analysis and Machine Intelligence*, 32(5) 861–874, 2010

[2] G Bao, S Hou, and P Li Imaging scattering by a continuation method with initial guesses from a direct imaging algorithm *J Comp Phys* , 227(1) 755–762, 2007

[3] S Belongie, J Malik, and J Puzicha Shape matching and object recognition using shape contexts *IEEE Transactions on Pattern Analysis and Machine Intelligence*, 24(4) 509–522, 2002

[4] F Cakoni and D Colton *Qualitative Methods in Inverse Scattering Theory An introduction* Berlin Springer, 2005

[5] K Chadan and P C Sabatier *Inverse Problems in Quantum Scattering Theory* Berlin Springer-Verlag, 1989

[6] T F Chan Active contours without edges *IEEE Transactions on Image Processing*, 10(2) 266–277, 2001

[7] M Cheney The linear sampling method and the music algorithm *Inverse Problems*, 17 591–595, 2001

[8] G C -H Chuang and C -C J Kuo Wavelet descriptor of planar curves Theory and applications *IEEE Transactions on Signal Processing*, 5(1) 56–70, 1996

[9] D Colton, J Coyle, and P Monk Recent developments in inverse acoustic scattering theory *SIREV*, 42 369–414, 2000

[10] D Colton and A Kirsch A simple method for solving inverse scattering problems in the resonance region *Inverse Problems*, 12 383–393, 1996

[11] D Colton and R Kress *Integral Equation Methods in Scattering Theory* New York Wiley-Interscience Publication, 1993

[12] D Colton and R Kress *Inverse Acoustic and Electromagnetic Scattering Theory* Berlin Springer, 1998

[13] A J Devaney Super-resolution processing of multi-static data using time-reversal and music *to appear in J Acoust Soc Am*

[14] L Gorelick, M Galun, E Sharon, R Basri, and A Brandt Shape representation and classification using the poisson equation *ACCV*, 28 1991–2005, 2006

[15] F K Gruber, E A Marengo, and A J Devaney Time-reversal imaging with multiplesignal classification considering multiple scattering between the targets *J Acoust Soc Am* , 115 3042–3047, 2004

[16] S Hou, K Huang, K Solna, and H -K Zhao A space and phase coherent direct imaging method *J Acoust Soc Am* , 125(1) 227–238, 2009

[17] S Hou, K Solna, and H -K Zhao Imagıng of locatıon and geometry for extended targets usıng the response matrıx *J Comp Phys* , 199(1) 317–338, 2004

[18] S Hou, K Solna, and H -K Zhao A dırect ımagıng algorıthm for extended target *Inverse Problems*, 22 1151–1178, 2006

[19] S Hou, K Solna, and H -K Zhao A dırect ımagıng method for far field data *Inverse Problems*, 23 1533–1546, 2007

[20] D S Jones *Acoustıc and Electromagnetıc Waves* Oxford Clarendon Press, 1986

[21] E Kerbrat, C Prada, D Cassereau, , and M Fınk Ultrasonıc nondestructıve testıng of scatterıng medıa usıng the decomposıtıon of the tıme reversal operator *IEEE Trans Ultrason , Ferroelec , Freq Contr* , 49(8), 2002

[22] E Kerbrat, C Prada, and M Fınk Imagıng ın the presence of graın noıse usıng the decomposıtıon of the tıme reversal operator *J Acoust Soc Am* , 113(3) 1230–1240, 2003

[23] A Kırsch The domaın derıvatıve and two applıcatıons ın ıverse scatterıng theory *Inverse Problems*, 9 81–96, 1993

[24] A Kırsch Charactorızatıon of the shape of a scatterıng obstacle usıng the spactral data of the far-field operator *Inverse Problems*, 14 1489–1512, 1998

[25] A Kırsch The music algorıthm and the factorızatıon method ın ınverse scatterıng theory for ınhomogenıous medıa *Inverse Problems*, 18 1025–1040, 2002

[26] R Kress Integral equatıon methods ın ınverse obstacle scatterıng *Engıneerıng Analysıs wıth Boundary Elements*, 15(2) 171–179, 1995

[27] R Kress On the numerıcal solutıon of a hypersıngular ıntegral equatıon ın scatterıng theory *Journal of Computatıonal and Applıed Mathematıcs*, 61 345–360, 1995

[28] L J Lateckı, R Lakamper, and U Eckhardt Shape descrıptors for non-rıgıd shapes wıth a sıngle closed contour *IEEE Conf on Computer Vısıon and Pattern Recognıtıon*, 15(2) 424–429, 2000

[29] P D Lax and R S Phıllıps *Scatterıng Theory* New York Academıc Press, 1967

[30] R Leıs *Inıtıal Boundary Value Problems ın Mathematıcal Physıcs* New York John Wıley, 1986

[31] I -J Lın and S Y Kung Codıng and comparıson of dags as a novel neural structure wıth applıcatıon to on-lıne handwrıtten recognıtıon *IEEE Transactıons on Sıgnal Processıng*, 45(11) 2701–2708, 1997

[32] F Mokhtarıan, S Abbası, and J Kıttler Effıcıent and robust retrıeval by shape content through curvature scale space *Image Databases and Multı-Medıa Search*, 1 51–58, 1997

[33] C Muller *Foundatıons of the Mathematıcal Theory of Electromagnetıc Waves* Berlın Heıdelberg New York Sprınger-Verlag, 1969

[34] R G Newton *Scatterıng Theory of Waves and Partıcles* Berlın Heıdelberg New York Sprınger-Verlag, 1982

[35] S Nı, P Wang, M Paun, W Daı, and A Paun Spotted cdna mıcroarray ımage segmentatıon usıng acwe *Romanıan Journal of Informatıon Scıence and Technology*, 12 249–263, 2009

[36] C Prada, S Mannevılle, D Spolıansky, and M Fınk Decomposıtıon of the tıme reversal operator Detectıon and selectıve focusıng on two scatterers *J Acoust Soc Am* , 99 2067–2076, 1996

[37] C Prada and J -L Thomas Experımental subwavelength localızatıon of scatterers by decomposıtıon of the tıme reversal operator ınterpreted as a covarıance matrıx *J Acoust Soc Am* , 114(1) 235–243, 2003

[38] C Prada, J -L Thomas, and M Fınk The ıteratıve tıme reversal process Analysıs of the convergence *J Acoust Soc Am* , 97(1) 62–71, 1995

[39] M Reed *Scatterıng Theory* New York Academıc Press, 1979

[40] R O Schmıdt Multıple emıtter locatıon and sıgnal parameter estımatıon *IEEE Trans Antennas Propagatıon*, 34(3) 276–280, 1986

[41] T Sebastıan, P Kleın, and B Kımıa On alıgnıng curves *IEEE Transactıons on Pattern Analysıs and Machıne Intellıgence*, 25(1) 116–125, 2003

[42] M Tanter and M Fink Real time inverse filter focusing by iterative time reversal *J Acoust Soc Am*, 115 768–775, 2004

[43] M Tanter and M Fink Revisiting iterative time reversal processing Application to detection of multiple targets *J Acoust Soc Am*, 115 776–784, 2004

[44] C H Wilcox *Scattering Theory for the d'Alembert Equation in Exterior Domains* Berlin Heidelberg New York Springer-Verlag Lecture Notes in Mathematics 442, 1975

[45] Y Xu, B Wang, W Liu, and X Bai Skeleton graph matching based on critical points using path similarity *ACCV*, 3 456–465, 2009